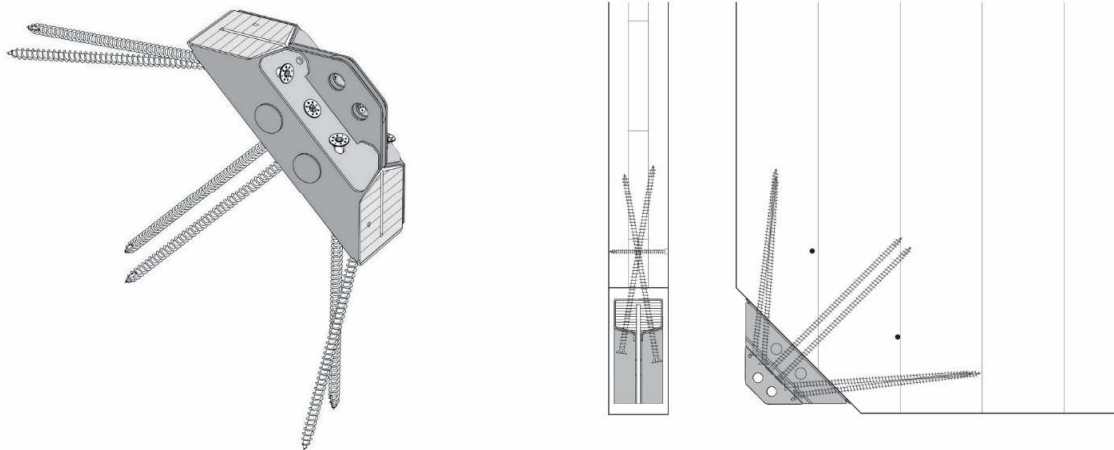


X-ONE CONNECTION - EXPERIMENTAL ANALYSIS

MECHANICAL BEHAVIOUR AND RESISTANCE DOMAIN

DEVELOPMENT OF AN INNOVATIVE CALCULATION MODEL FOR TIMBER
BUILDINGS USING THE X-RAD SYSTEM



The original document is written in Italian. Versions in other languages derive from this original document

10/2015

CONTENTS

1. INTRODUCTION	4
2. DESCRIPTION OF THE CONNECTION	5
2.1. BASIC COMPONENTS	5
2.1.1. External box	6
2.1.2. LVL insert	8
2.1.3. Internal stiffening plate	8
2.1.4. $\varnothing 12$ Bolts	8
2.1.5. VGS full thread screws	9
2.2. CHARACTERISTICS OF THE MATERIALS	10
2.2.1. LVL wood (Laminated Veneer Lumber)	10
2.2.2. Steel	10
3. INPUT DATA	11
3.1. TESTS CONDUCTED AT THE TU-GRAZ CENTER	11
3.1.1. Monotonic tests along the Y-axis	11
3.1.2. Monotonic tests along the X-axis	13
3.2. TESTS CONDUCTED AT THE CNR-IVALSA CENTER (SAN MICHELE A.A.)	14
3.2.1. Cyclic tests along the Y-axis	14
3.2.2. Cyclic tests along the X-axis	15
3.3. TESTS CONDUCTED AT THE UNIVERSITY OF TRENTO	16
3.3.1. Single panel tests	16
3.3.2. Composite panel tests	18
3.4. FEM ANALYSIS	19
3.4.1. Case studies	20
3.4.2. Main results	21
4. ANALYSIS OF THE VARIOUS STRESS CONDITIONS	25
4.1. COORDINATE SYSTEMS AND DEFINITIONS	25
4.2. SUMMARY OF THE EXPERIMENTAL DATA AVAILABLE UNTIL NOW	26
4.3. FAILURE MODE OF THE CONNECTION	27
4.3.1. Shear-Tension ($\alpha=0^\circ$)	30
4.3.2. 45 degree tension ($\alpha=45^\circ$)	30
4.3.3. Tension ($\alpha=90^\circ$)	30
4.3.4. 45 degree shear ($\alpha=135^\circ$ or $\alpha=315^\circ$)	30
4.3.5. Shear-Compression ($\alpha=180^\circ$)	31
4.3.6. 45 degree compression ($\alpha=225^\circ$)	31
4.3.7. Compression ($\alpha=270^\circ$)	31
4.4. FAILURE ASSESSMENT	31
4.4.1. Shear-Tensile stress ($\alpha=0^\circ$)	32
4.4.2. 45 degree tension ($\alpha=45^\circ$)	33
4.4.3. Tension ($\alpha=90^\circ$)	34
4.4.4. 45 degree shear ($\alpha=135^\circ$ or $\alpha=315^\circ$)	34
4.4.5. Shear-Compression ($\alpha=180^\circ$)	36
4.4.6. 45 degree compression ($\alpha=225^\circ$)	36

4.4.7.	Compression ($\alpha=270^\circ$)	37
5.	DEFINITION OF A RESISTANCE CRITERION	38
5.1.	CONSTRUCTION OF THE FAILURE DOMAIN	38
5.1.1.	Domain based on experimental resistances.....	38
5.1.2.	Domain based on resistances by FEM modeling	40
5.1.3.	Comparison of experimental data with FEM modeling.....	40
5.1.4.	Domain based on the resistances by analytical failure calculation.....	42
5.1.5.	Comparison of experimental data with failure calculations	43
5.1.6.	Graphical interpretation of the domain	44
5.2.	FAILURE DOMAIN FOR THE ENGINEERING DESIGNER.....	44
5.2.1.	Field of use of the connection.....	47
5.2.2.	Characteristic failure domain	47
5.2.3.	Design failure domain	49
5.3.	DESIGN PROVISIONS AS PER EUROPEAN TECHNICAL APPROVAL (ETA- 15/0632).....	51
5.3.1.	Splitting	52

1. INTRODUCTION

The following technical report has been drafted by the company Rotho Blaas s.r.l. in order to provide details regarding the structure of the new connection system called "X-ONE". In view of its innovative character, it has been subjected to a set of laboratory tests, backed by finite element analyses. The laboratory tests were used as starting point for the drafting of this report that provides a series of considerations and of analytical formulations that should help in defining a criterion for assessing the connection. This report, in fact, provides an assessment criterion for only the X-ONE element of the X-RAD system and of the element's full thread VGS screws that connect it to the CLT panel. The system's other components, such as the external plates X-PLATE, have been excluded from the report.

The purpose of this report is to supply the structural designer with a theory-based guide for assessing the connection. In no circumstance can this report be used for any other purpose without the authorization of the Rotho Blaas company. In any case, as indicated also in the connection's European Technical Approval document (ETA), the designing of X-RAD based connections must be carried out under the responsibility of an engineer experienced in timber structure construction (ETA 15/0632 §2.2).

Chapter 2 provides a description of the connection and of the materials it is made of.

Chapter 3 gives a short summary of the key data available, such as the outcomes of the lab tests and of the FEM simulations.

Chapter 4 describes the analysis made of the various stress conditions the connection can be subjected to. The various considerations are based on experimental data as well as on analytical diagrams.

Chapter 5 provides the development of a resistance criterion for the analytical analysis of the connection, given the values of the stress forces. The resistance criterion has been developed starting from the analytical calculations, supported by the available experimental investigations matched up with the results deriving from Finite Element Method (FEM) modeling.

2. DESCRIPTION OF THE CONNECTION

The X-ONE connector consists of an external steel box (1), containing an LVL wood insert and an internal plate (2), both of which are connected to the external box via two $\varnothing 12$ bolts. The external plate and the external box are fastened to external plates, called X-PLATES, via two $\varnothing 16$ bolts, so as to form the complete X-RAD system. Connection with the CLT panel is ensured by means of 6 full thread VGS screws inserted at various inclinations.

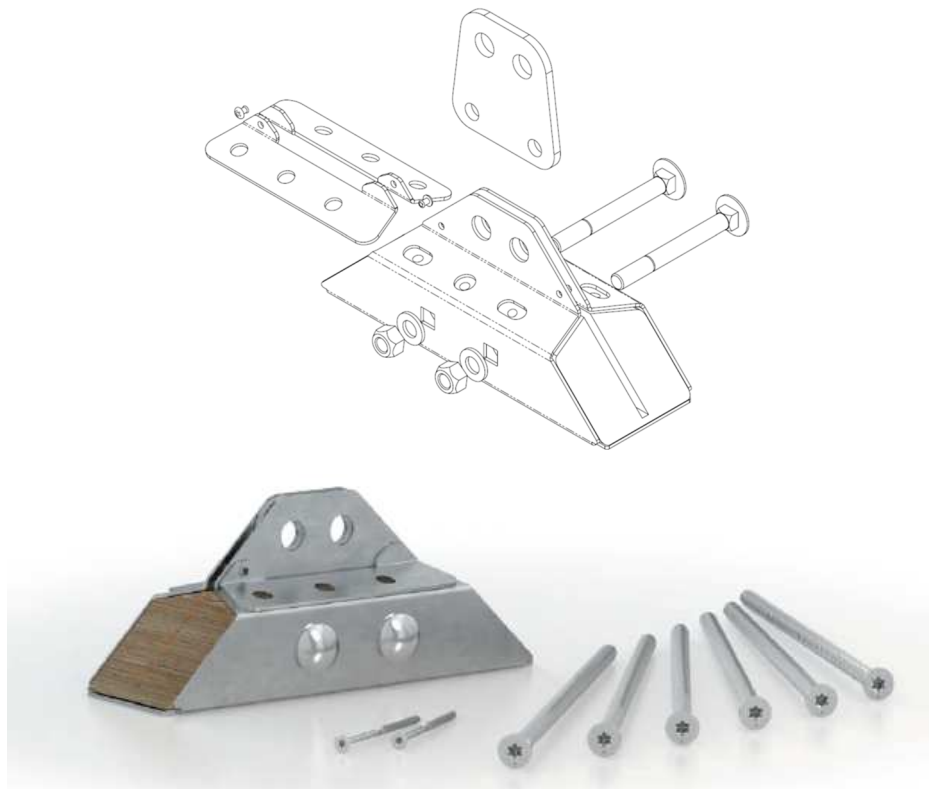


Figure 1: Exploded view of the connection

2.1. Basic components

As indicated above, the X-RAD connection system consists of the following three basic components:

1. **X-ONE:** a pre-assembled element consisting of the following parts:
 - An external box, consisting of a folded metal element that wraps around the LVL insert, which is mainly invested by bearing stresses in correspondence with the points of connection of the bolts with the external plate;
 - an LVL insert, subjected to compression stress orthogonally to the fibre and to bearing stress by the internal bolts;
 - an internal plate connected to the external plate and to the metal box via the two external bolts;

- 2 internal $\varnothing 12$ bolts that connect the internal plate to the LVL insert, thus creating a wood-steel-wood shear connection.
2. **6 FULL THREAD VGS SCREWS** loaded axially and in shear, that achieve the wood-to-wood connection between the CLT panel and the LVL insert of the X-ONE.
 3. **EXTERNAL X-PLATES:** steel plates that allow to connect the X-ONE to the ground or to the mutual X-ONE/X-ONE connection; a whole set of plates has been designed for the most diverse geometric configurations. The external plates are connected to the X-ONE by 2 $\varnothing 16$ bolts.

Following are pictures of the various components.



Figure 2: Front and side views of the X-ONE



Figure 3: Components of the X-RAD system

2.1.1. External box

It consists of a DX51D steel, or equivalent, bent plate having the following geometric features.

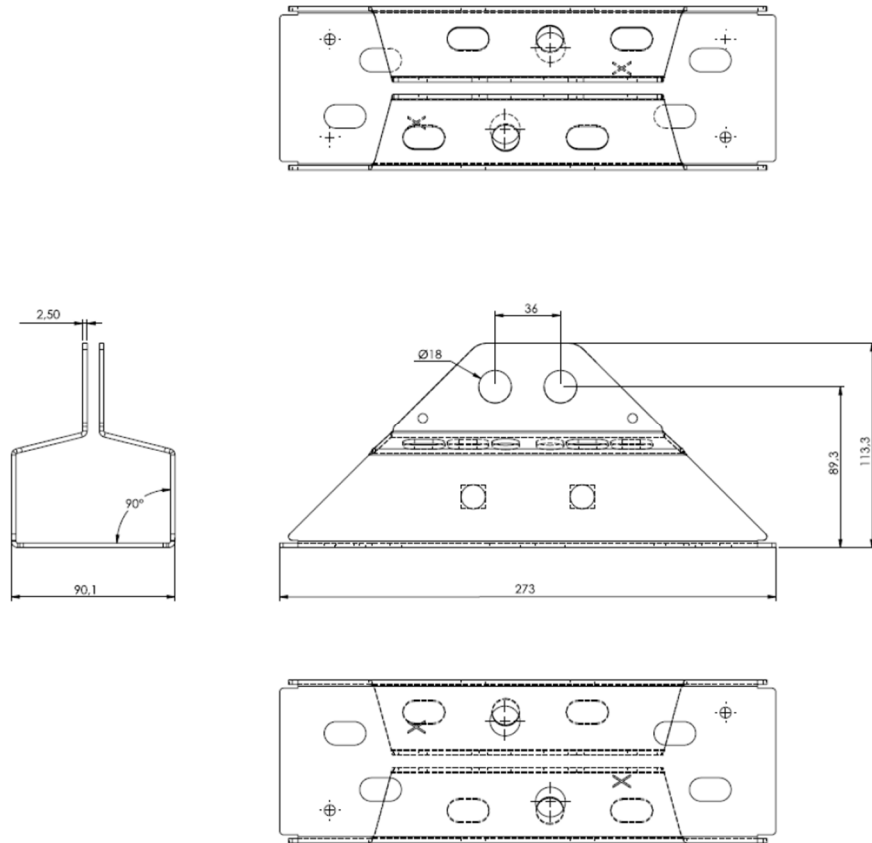


Figure 4: External steel box.

An additional metal plate cover is provided to be placed in the position where the full thread screws are inserted. Its purpose is to reinforce the plate so as to prevent screw head penetration due to metal plate punching.

Steel cover

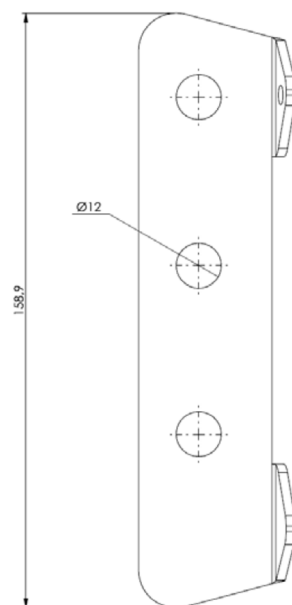


Figure 5: Additional metal cover for the external box.

2.1.2. LVL insert

The LVL wooden insert is shaped like the external box and inserted inside it. The insert has a central slot made to house the internal plate and is predrilled to receive the $\varnothing 12$ bolts. It also has 6 pre-drilled holes for the insertion of the VGS full thread screws and 2 pre-drilled holes for the HBS positioning screws used during assembly.

2.1.3. Internal stiffening plate

It consists of a DX51D steel, or equivalent, plate having the following geometric features

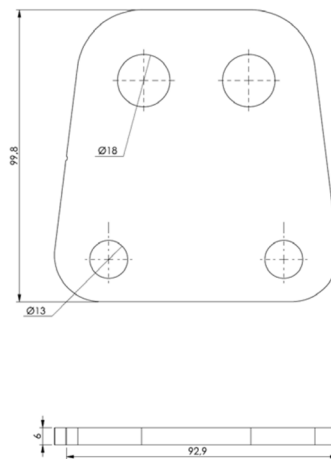


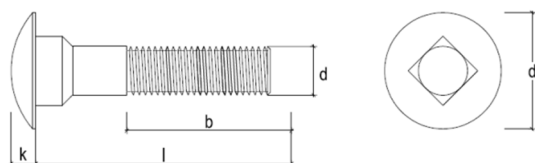
Figure 6: Internal plate

2.1.4. $\varnothing 12$ Bolts

The $\varnothing 12$ bolts connecting the external box, the LVL insert and the internal stiffening plate, have the following geometrical and mechanical features.

Bolt 8.8 M12x110 mm	
Tensile strength	$\geq 600 \text{ N/mm}^2$
E-Modulus	210 000 N/mm ²
Head diameter d_k	30.65 mm
Head height k	6.95 mm
Nominal diameter d	12 mm
Length l	110 mm
Threaded length b	30 mm
Pitch	1.75 mm

Bolt



Special nut	
Thread diameter d	M12
Head dimension sw	24 mm
Head thickness t	5 mm
Height h	15 mm
Outer diameter D	18 mm

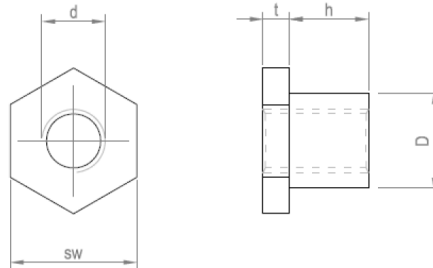


Figure 7: Features of the Ø12 bolts

2.1.5. VGS full thread screws

The connection includes 6 full thread VGS screws, of which some of the main characteristics are reported here under.

GEOMETRY AND MECHANICAL CHARACTERISTICS			
VGS CONNECTOR			
Nominal diameter	d _n [mm]	9	11
Head diameter	d _k [mm]	16,00	19,30
Tip diameter	d _j [mm]	5,90	6,60
Shank diameter	d _s [mm]	6,50	7,70
Head thickness	t ₁ [mm]	6,50	8,20
Pre-bored hole diameter *	d _v [mm]	5,0	6,0
Characteristic yield moment	M _{y,k} [Nmm]	27244,1	45905,4
Characteristic extraction-resistance parameter	f _{ax,k} [N/mm ²]	11,7	11,7
Characteristic tensile strength	f _{tens,k} [kN]	25,4	38,0
Characteristic yield strength	f _{y,k} [N/mm ²]	1000	1000

(*) Pre-bored hole required for connectors with Ø11 ≥ 400 mm

As will be seen further on, in the event of these screws being subjected to tension, the screw shaft breaks because:

- the screw's insertion depth into the CLT is enough to mobilize the entire shaft's tensile strength;
the metal external box and stiffening plate act as "washers", distributing the load over a greater surface and causing failure by tension of the screw.

The characteristic tensile strength of the Ø11 VGS screw is equal to:

$$f_{tens,k} = 38,0 \text{ kN}$$

In the event of compressive stress, the resistant mechanism corresponds to that of the screw's thread. In this case, the tests performed at CNR-IVALSA have shown a mean withdrawal strength of the thread in the LVL equal to:

$$f_{comp,k} = 35,0 \text{ kN}$$

2.2. Characteristics of the materials

2.2.1. LVL wood (Laminated Veneer Lumber)

The insert inside the metal box consists of laminated veneer lumber (LVL) with typical density $\rho_k \geq 680 \text{ kg/m}^3$

2.2.2. Steel

The following steel plates are present:

- External box, consisting of bent plate, 2.5 mm thick;
- Internal stiffening plate, 6 mm thick.

The two plates are made of DX51D steel as per EN 10346 or equivalent.

DX51D steel is manufactured at the following standards:

- EN 10346:2009 – Continuously hot-dip coated steel flat products – Technical delivery conditions.
- EN 10143:2006 – Continuously hot-dip coated steel sheet and strip. Tolerances on dimensions and shape.

The minimum mechanical characteristics of steel are provided in Table 6 of EN 10346:2009:

Table 6 — Mechanical properties (transverse direction) of low carbon steels for cold forming

Designation			Yield strength	Tensile strength	Elongation	Plastic strain ratio	Strain hardening exponent
			R_e^a	R_m	A_{80}^b	r_{90}	n_{90}
Steel grade		Symbols for the types of available coatings	MPa	MPa	%	min.	min.
Steel name	Steel number						
DX51D	1.0226	+Z,+ZF,+ZA,+AZ,+AS	–	270 to 500	22	–	–

Figure 8: Excerpted from EN 10346:2009

As regards the definition of the strengths to be used during calculation, for safety purposes the strengths relating to S275 steel (EN 10025) are considered, that are anyhow lower than the actual strengths derived from the experimental investigations conducted on the metal sheets:

$$R_{u,k} = 410 \text{ MPa}$$

$$R_{y,k} = 275 \text{ MPa}$$

3. INPUT DATA

Following is a brief description of the input data used to develop this technical report.

The laboratory tests were conducted in three different research centers:

- *Lignum Test Center* of the University of Graz (TU-GRAZ).
- *Trees and Timber Institute* of San Michele All'Adige (CNR-IVALSA).
- *Environmental and Mechanical Civil Engineering Department* of the University of Trento.

At the Lignum Test Center of the University of Graz, Austria, monotonic tests were conducted according to standard EN 26891:1991. The purpose of the tests was to identify the parameters to be used for the compilation of the European Technical Approval (ETA 15/0632). In accordance with the TU-GRAZ center, a campaign of cyclic tests was conducted at the CNR-IVALSA center, in Italy, in compliance with the standard EN 12512:2006. The purpose of these tests was to define the ductility of the connection and its behaviour from a seismic perspective, which information is also contained in the ETA document of reference.

The purpose of the investigations conducted at the University of Trento, Italy, was to test the overall wall-connection system and its global behaviour.

The laboratory tests were integrated with an FEM analysis campaign of the connection.

3.1. Tests conducted at the TU-GRAZ center

At the Lignum Test Center of the University of Graz, monotonic tests were conducted in accordance with EN 26891, in both tension and shear configurations. Following are the test diagrams and the main outcomes of the two stresses applied, i.e. tension and shear.

The tests were conducted along the two main axes, x and y.

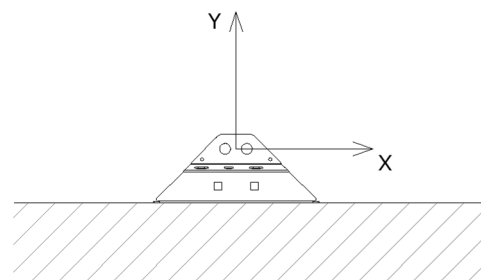


Figure 9: Local reference system of the X-RAD

3.1.1. Monotonic tests along the Y-axis

Following is a schematic rendition of the test set-up.

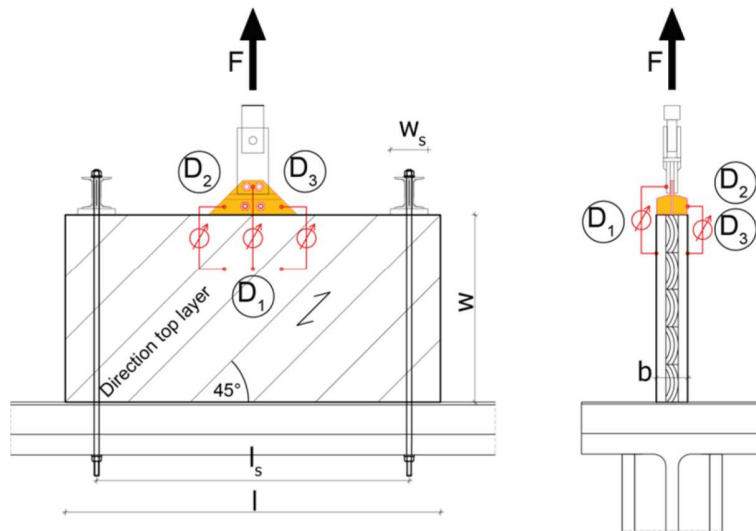


Figure 10: Diagram of the test along the y-axis

The test report provides the rigidity and characteristic resistance values of the connection in the two configurations.

The following figure shows the Force-Displacement curves for the tests along the y-axis.

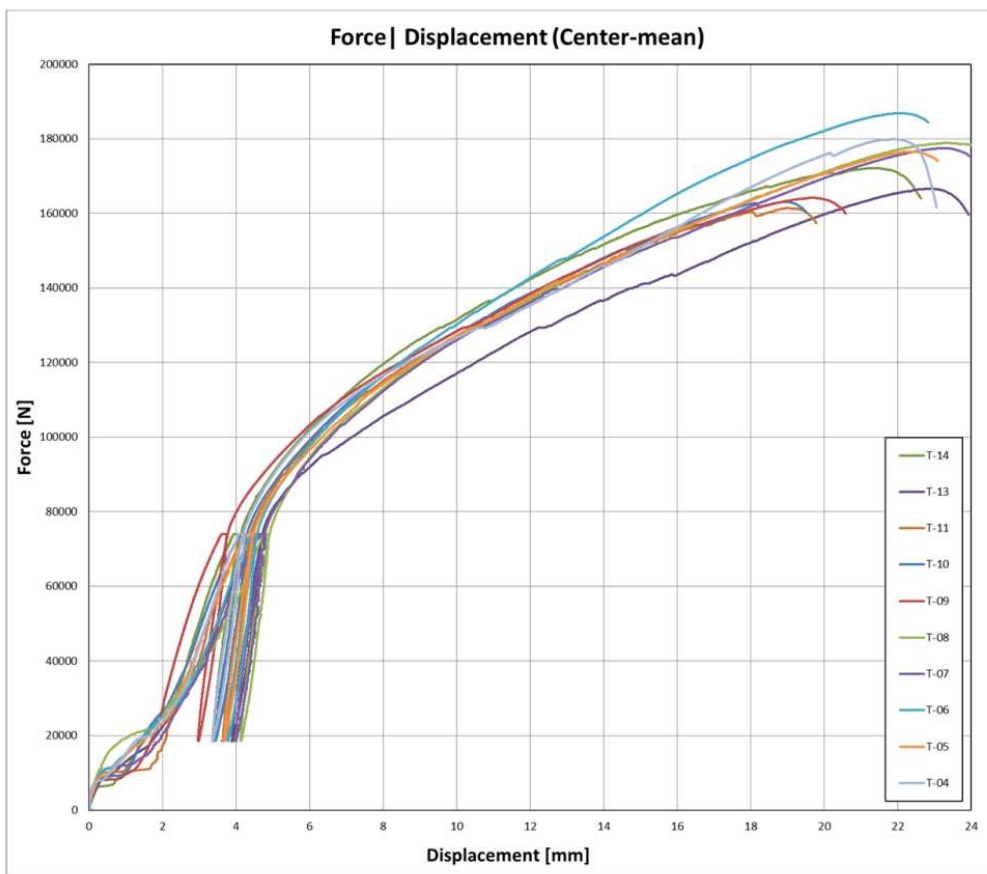


Figure 11: Force-Displacement curves for the tests along the y-axis

3.1.2. Monotonic tests along the X-axis

Below is the diagram showing the test set-up.

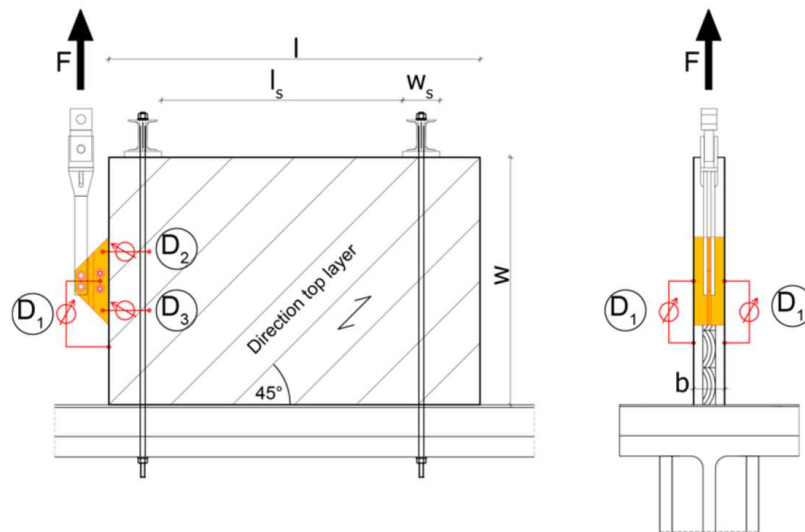


Figure 12: Diagram of the test along the x-axis

The test report provides the rigidity and characteristic resistance values of the connection.

The following figure shows the Force-Displacement curves for the tests along the x-axis.

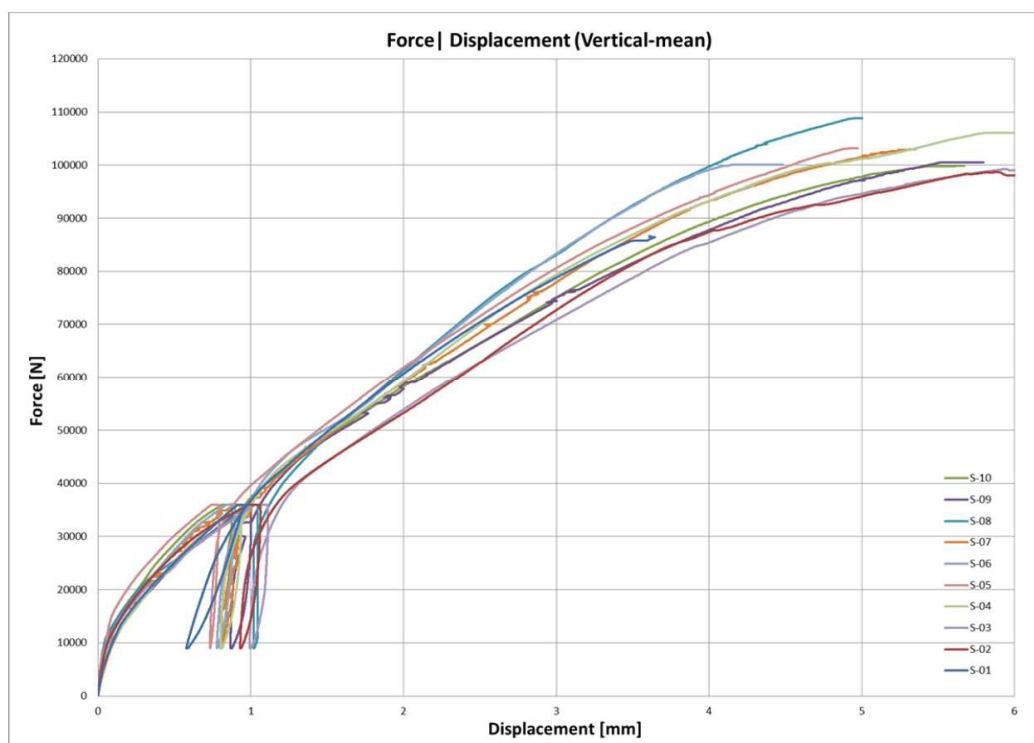


Figure 13: Force-Displacement curves for the tests along the x-axis

3.2. Tests conducted at the CNR-IVALSA center (San Michele A.A.)

At the laboratories of the CNR-IVALSA center of San Michele All'Adige, the following tests were conducted:

- **Full thread screw withdrawal testing:** testing of the various types of full thread VGS screws inserted in different types of hard woods, in order to define the most suitable screw-wood combination and therefore establish the best kind of wood in terms of mechanical behaviour.
- **Monotonic and cyclic tests on the X-ONE connection:** the tests were conducted in different phases of the system's development (from prototype to final version) in order to optimise its geometries and mechanical behaviour. The cyclic tests along the x-axis and along the y-axis were conducted in compliance with standard EN 12512.

3.2.1. Cyclic tests along the Y-axis

Below is a rendition of the test geometry.

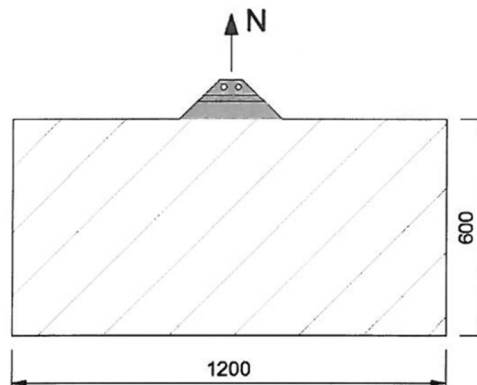


Figure 14: Diagram of the tests along the y-axis

The test report provides the resistance, displacement and ductility values.

Figure 15: Key results of the tests along the y-axis

By way of example, a Force-Displacement curve is shown.

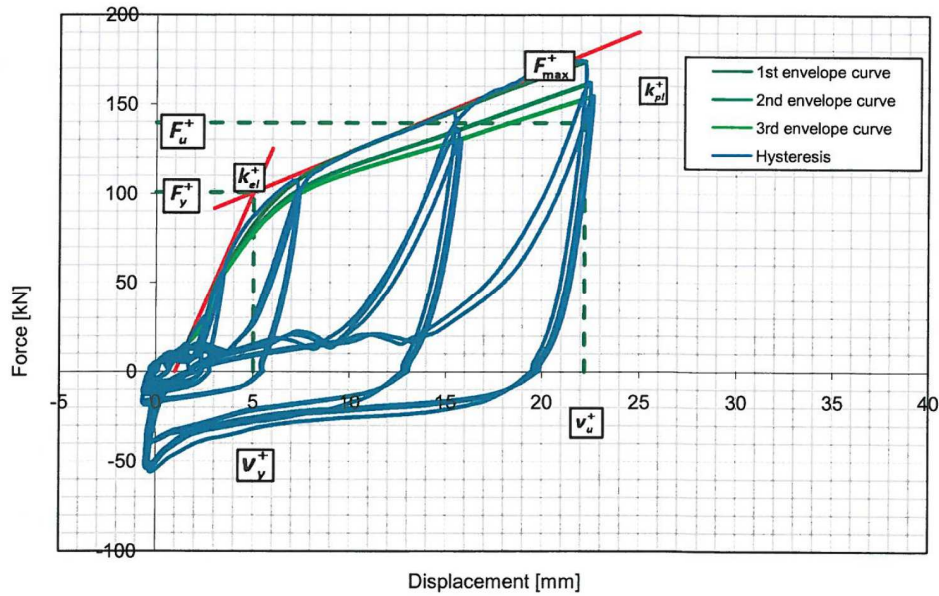


Figure 16: Force-Displacement diagram for one of the tests along the y-axis

3.2.2. Cyclic tests along the X-axis

Below is a rendition of the test geometry.

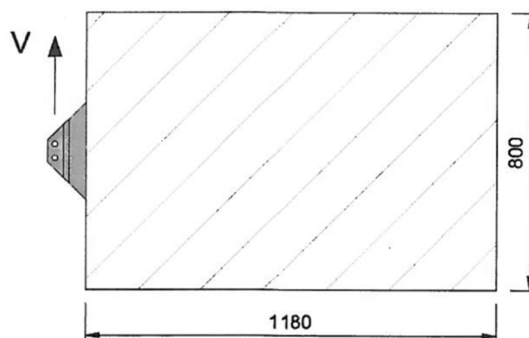


Figure 17: Diagram of the test along the x-axis

The test report provides the resistance, displacement and ductility values.

By way of example, a Force-Displacement curve is shown.

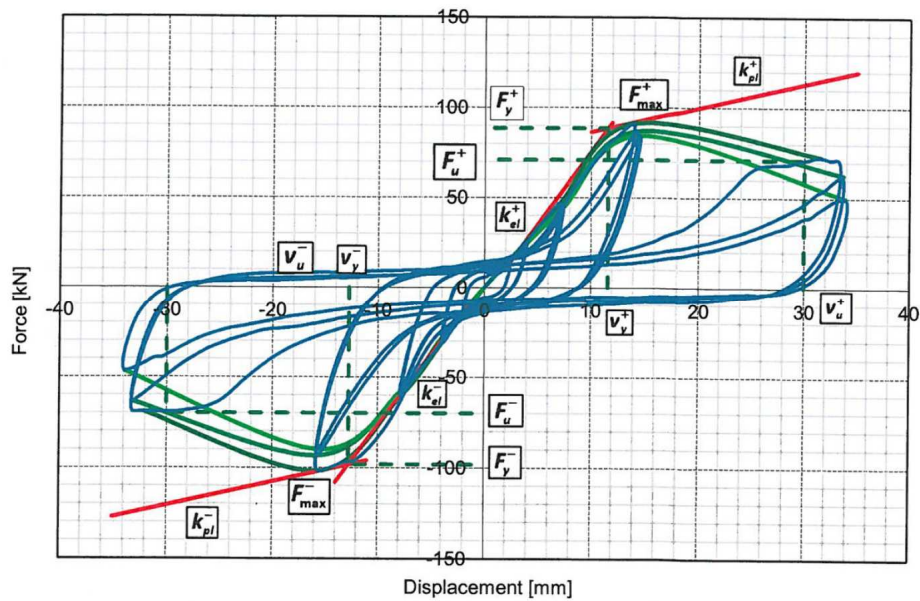


Figure 18: Force-Displacement diagram for one of the tests along the x-axis

3.3. Tests conducted at the University of Trento

At the Environmental and Mechanical Civil Engineering Department of the University of Trento, three tests on two samples, consisting of CLT panels connected using the X-RAD system, were conducted. The tests were conducted on two different configurations. The first configuration consisted of a CLT panel with two X-RAD elements fitted on the corners; the second configuration consisted of four CLT elements interconnected at their four corners using X-RAD connections.

3.3.1. Single panel tests

Here below is a representation of the test set-up, in which the 250 cm x 250 cm wall was fastened to the ground using two X-RAD connections and had a hydraulic jack fastened to the top of the panel that applied the displacement. The 20 kN/m² vertical load was applied to the wall using a lever system capable of maintaining the vertical load constant throughout the test. Two tests - a monotonic test and a cyclic test - were conducted on the panel in this configuration.



Figure 19: Single panel test set-up

Following is the graph showing the hydraulic jack's Force-Displacement diagram.

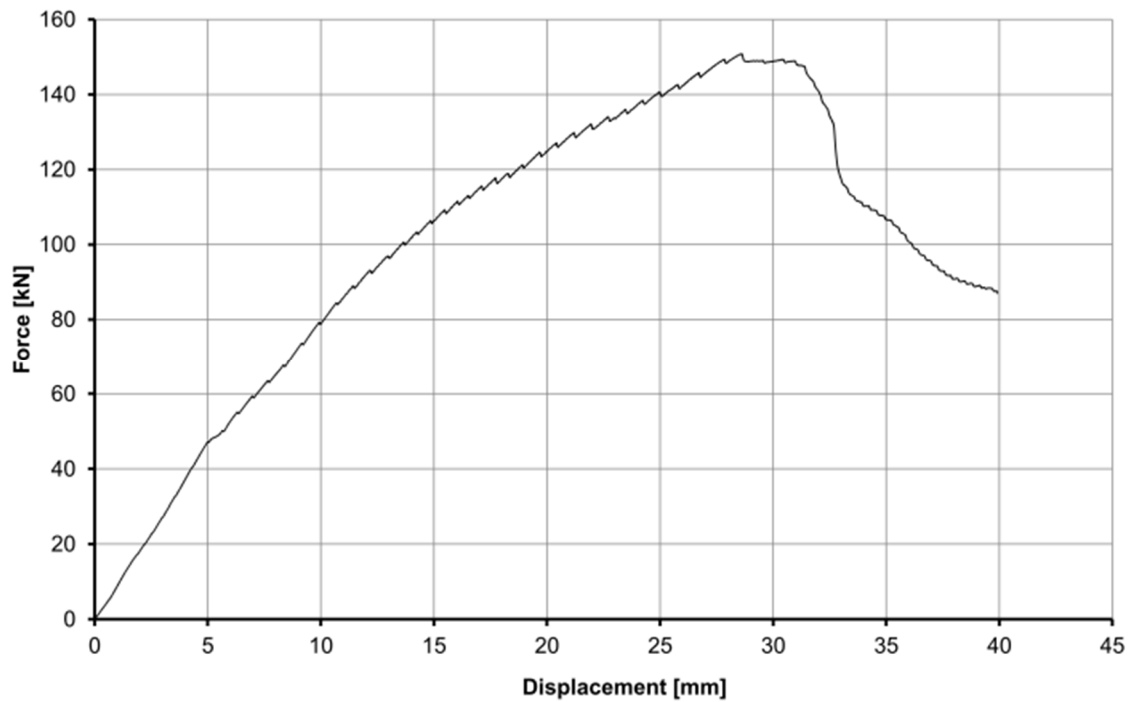


Figure 20: Force-Displacement diagram for the monotonic test

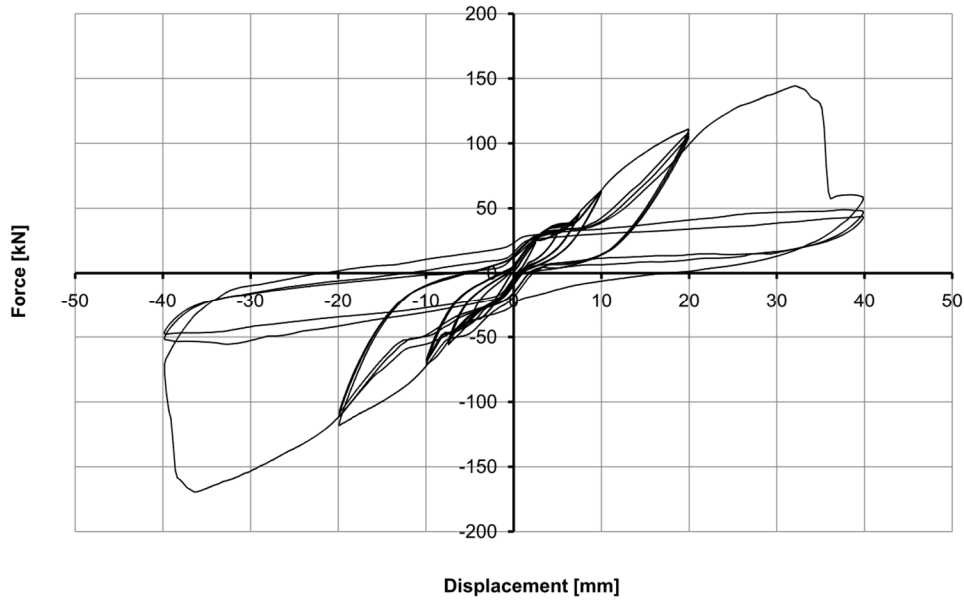


Figure 21: Force-Displacement diagram for the cyclic test

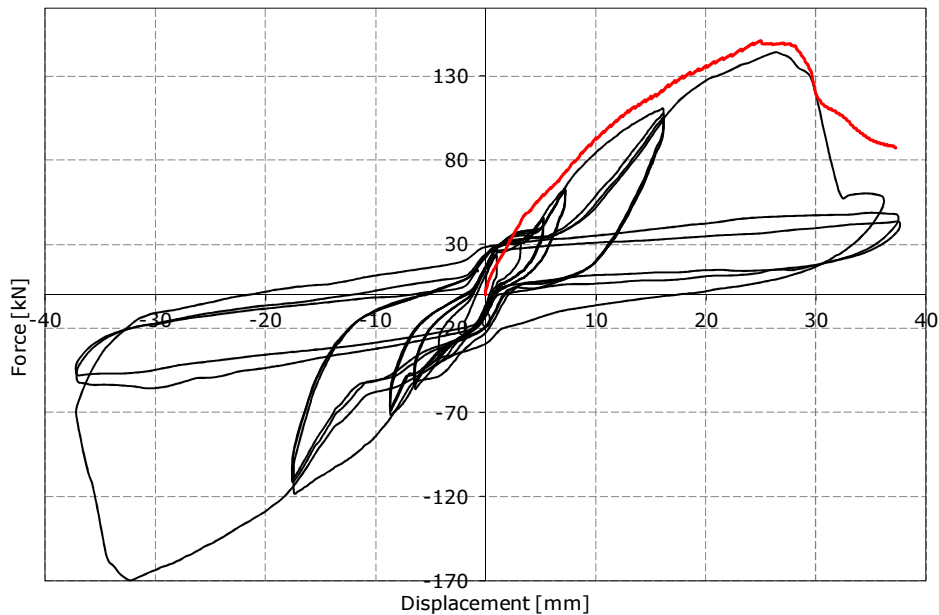


Figure 22: Superimposition of the Force-Displacement curves

3.3.2. Composite panel tests

Following is a representation of the test set-up, in which the wall was divided into four 125 cm x 125 cm panels interconnected using X-RAD connections. Like in the previous tests, a hydraulic jack was used to apply displacement. The vertical load on the wall, amounting to 20 kN/m², was applied using a lever capable of maintaining the vertical load constant throughout the test. One cyclic test was conducted on the sample in this configuration.

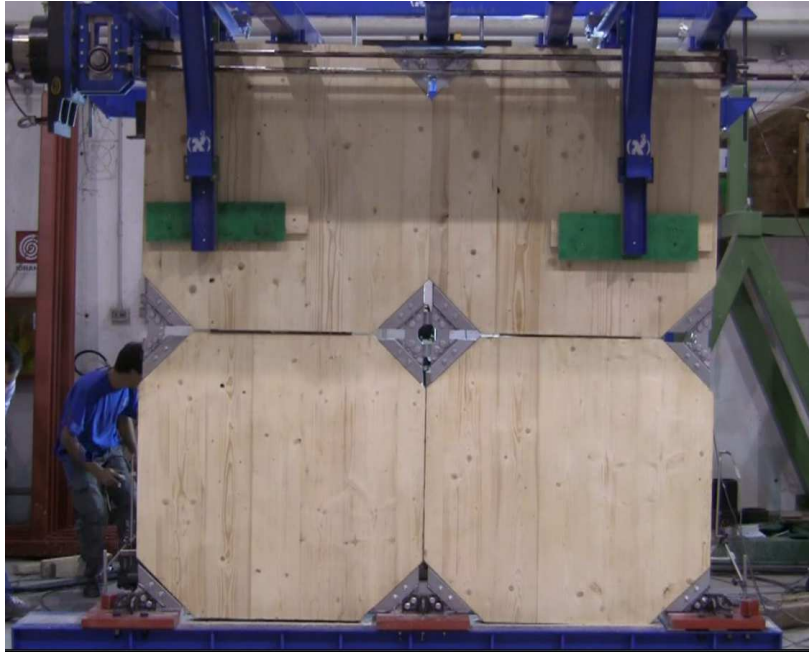


Figure 23: Test set-up for the wall divided into four sections

3.4. FEM analysis

A campaign of FEM simulations of the connection was conducted in order to better understand the various internal mechanisms affecting the overall behaviour of the connection and to obtain information regarding the behaviour of the connection when subjected to displacements along various directions.

The FEM model was calibrated on the tests conducted at the CNR-IVALSA in the two directions X and Y. Following is the image of a FEM model.

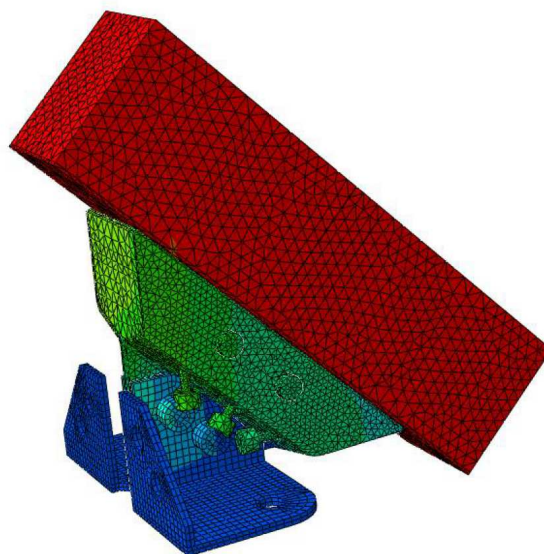


Figure 24: FEM model

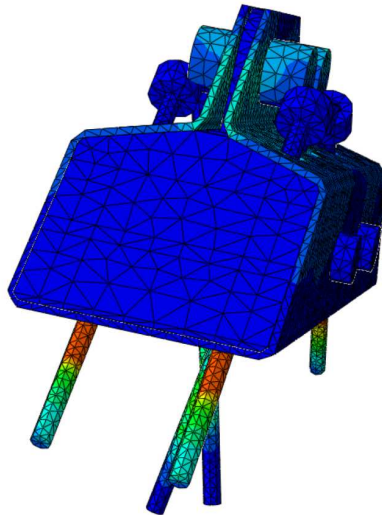


Figure 25: FEM image

3.4.1. Case studies

Eleven simulations were conducted, each one in a different displacement application direction. Consequently, eleven pushover analyses were conducted, applying a displacement along the directions shown in the following figure.

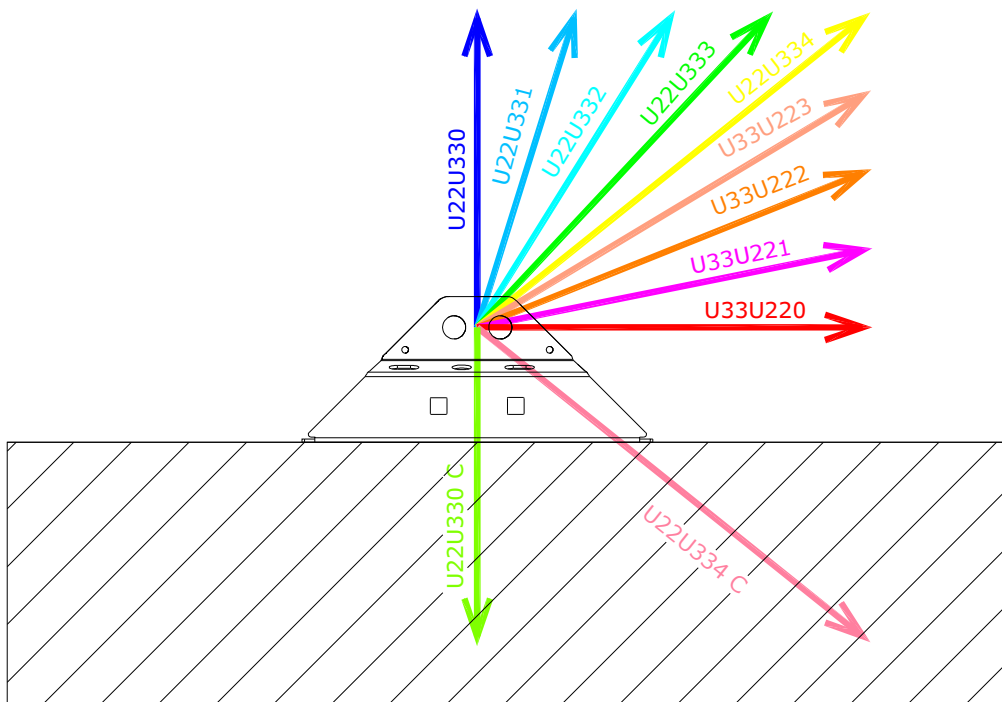


Figure 26: Displacement vectors applied to the FEM

3.4.2. Main results

A Force-Displacement diagram (capacity curve), such as the one shown here below, was plotted for each simulation. The capacity curves were then transformed by bi-linearization.

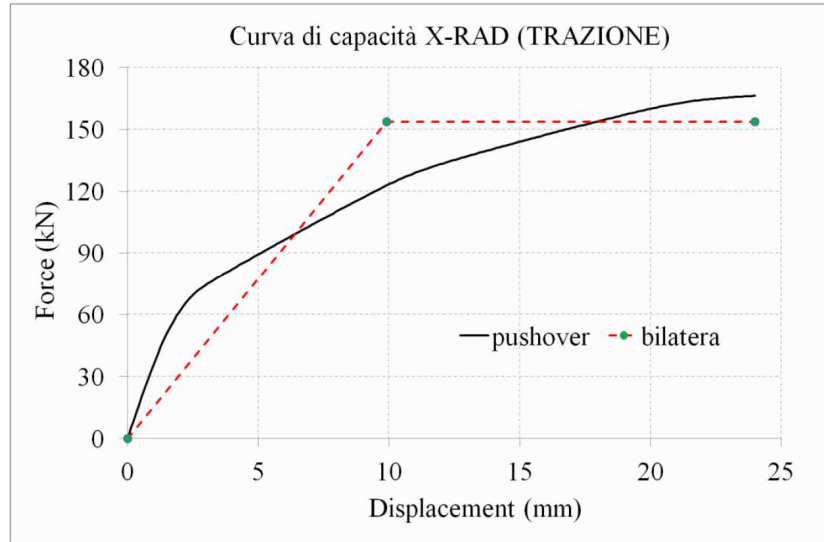


Figure 27: Example of capacity curve, with equivalent bi-linearization

Curva di capacità =X-RAD capacity curve (TENSION)

Bilatera = bilinear curve

The following table shows, for each analysis:

- F_{max} , equivalent to the maximum resistance derived from the capacity curve;
- u_{max} , equivalent to the maximum displacement of the capacity curve;
- F_y , equivalent to the yield strength of the equivalent bilinear curve;
- u_y , equivalent to the yield displacement of the equivalent bilinear curve;
- k_y , equivalent to the flexural rigidity of the equivalent bilinear curve;
- D , equivalent to the ductility of the equivalent bilinear curve.

PARAMETRI DELLE BILATERE							
Prova numerica	F_{max}	u_{max}	F_y	u_y	k_y	D	
	kN	mm	kN	mm	kN/mm	-	
Prev. Trazione	U22U330	166,22	24,00	153,62	9,91	15,50	2,42
	U22U331	161,66	25,14	153,62	10,68	14,38	2,35
	U22U332	151,71	28,30	153,62	12,81	11,99	2,21
	U22U333	136,23	32,89	126,14	9,55	13,21	3,44
	U22U334	126,18	38,42	117,54	9,43	12,46	4,07
Prev. Taglio	U33U223	118,78	30,02	109,27	8,75	12,49	3,43
	U33U222	116,90	32,31	108,50	9,90	10,96	3,26
	U33U221	110,92	30,59	103,06	9,62	10,71	3,18
	U33U220	104,99	30,00	99,47	10,09	9,86	2,97
Prev. Compr.	U22U334 C	233,63	38,42	209,75	6,24	33,62	-
	U22U330 C	247,26	24,00	225,85	5,24	43,08	-

Figure 28: Parameters of the bilinear curves

Legenda:

PARAMETRI DELLE BILATERE = Parameters of the bilinear curves

Prova numerica = Numerical test

Prev. Trazione = Prev. Tension

Prev. Taglio = Prev. Shear

Prev. Compr. = Prev. Compr.

The following picture shows the various bilinear curves and their parameters.

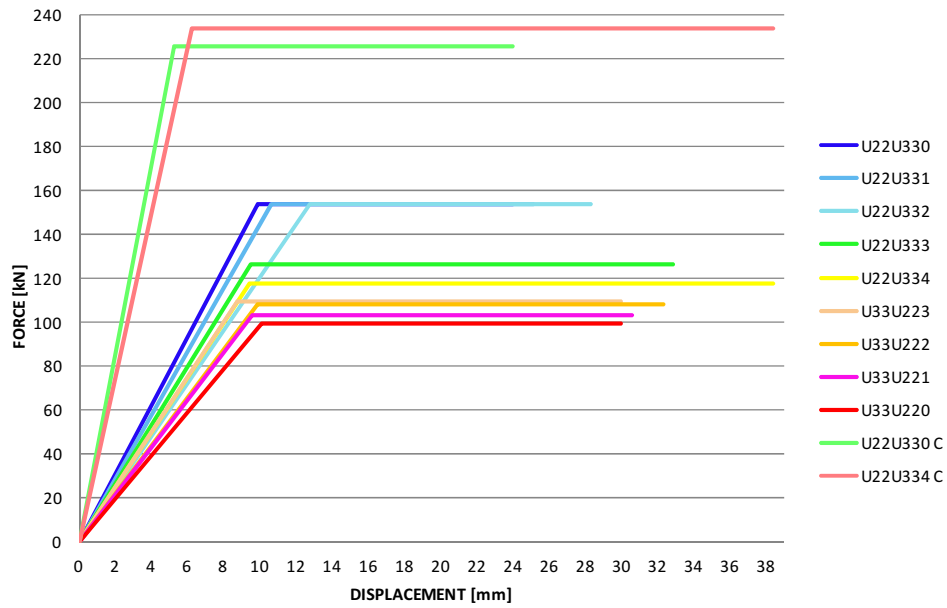


Figure 29: Bilinear curves

Within the FEM models the maximum resistance values of the two stress components were derived; the following table shows the resulting values.

	Fx [kN]	Fy [kN]
U22U330	0,00	166,22
U22U331	13,19	161,43
U22U332	29,93	149,79
U22U333	51,52	126,24
U22U334	80,86	97,02
U33U223	90,24	77,24
U33U222	99,83	60,83
U33U221	103,92	38,76
U33U220	104,99	0,00
U22U334 C	110,55	-205,82
U22U330 C	0,00	-247,26

Figure 30: Projection of the maximum resistances in the x-y plane

where the x-y reference system is shown in the figure.

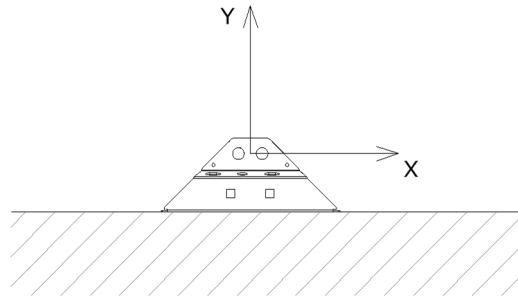


Figure 31: Local reference system of the X-RAD

At this point, it was possible to graphically plot the representative points of the various simulations in the x-y plane.

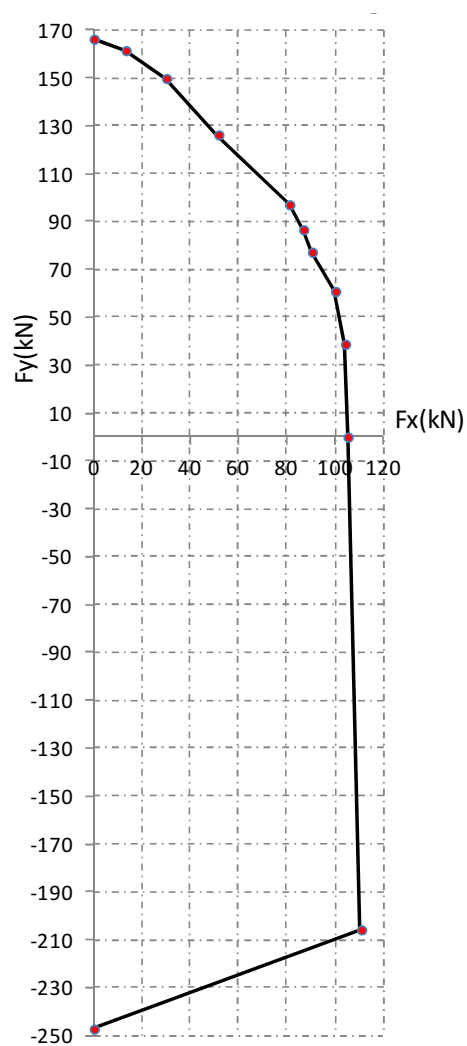


Figure 32: Shear-tension interaction domain derived from the FEM simulations

4. ANALYSIS OF THE VARIOUS STRESS CONDITIONS

Based on the results obtained from the laboratory tests and FEM analyses, following is a study on the behaviour of the connection in various stress conditions.

4.1. Coordinate systems and definitions

For the purposes of this study, a conventional reference system has been adopted in which the stresses applied to the X-RAD are defined as follows:

- TENSION: a vertical force directed along the positive z-axis, that therefore tends to make the full thread screws work under tension.
- COMPRESSION: a vertical force directed along the negative z-axis, that therefore tends to make the full thread screws work under compression.
- SHEAR-TENSION: a horizontal force directed along the positive x-axis, that therefore tends to make the full thread screws work under tension.
- SHEAR-COMPRESSION: a horizontal force directed along the negative x-axis, that therefore tends to make the full thread screws work under compression.

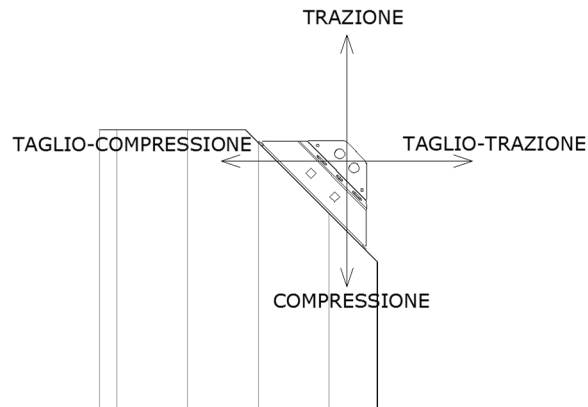


Figure 33: Stresses applied to the X-RAD in the CLT wall reference system

TRAZIONE = TENSION

TAGLIO-COMPRESSIONE = SHEAR-COMPRESSION

COMPRESSIONE = COMPRESSION

TAGLIO-TRAZIONE = SHEAR-TENSION

Considering the system's symmetry, the following observations can be made:

- In the X-RAD system, tension is equivalent to shear-tension.
- In the X-RAD system, compression is equivalent to shear-compression.

In addition to the four stresses considered above, it is necessary to define another four stresses, indicated as follows.

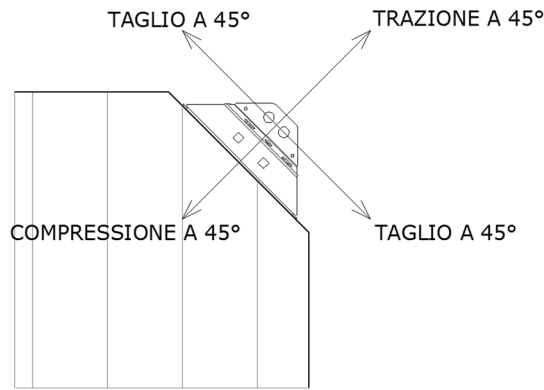


Figure 34: Stresses applied to the X-RAD in the CLT wall reference system

TAGLIO A 45° = 45 DEGREE SHEAR

TRAZIONE A 45° = 45 DEGREE TENSION

COMPRESSIONE A 45° = 45 DEGREE COMPRESSION

It should be noted that the 45 degree shear and the 45 degree tension stresses correspond to the X and Y directions, respectively, tested in the laboratory.

In the reference system of the CLT wall, the eight stresses indicated above had the following inclinations, when measuring the angles counter clockwise starting from the x-axis.

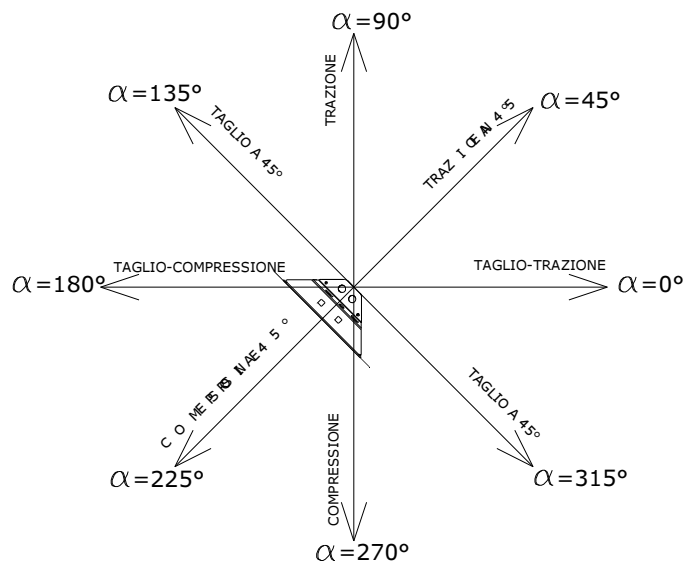


Figure 35: Stresses applied to the X-RAD in the CLT wall reference system

TAGLIO A 45° = 45 DEGREE SHEAR

TRAZIONE A 45° = 45 DEGREE TENSION

COMPRESSIONE A 45° = 45 DEGREE COMPRESSION

4.2. Summary of the experimental data available until now

As indicated in the previous chapters of this report, the single panel has been subjected to many tests. Following is a summary of the more significant results:

Sollecitazione	Angolo	Note	F _k [kN]	F _{min} [kN]	F _{mean} [kN]	F _{max} [kN]	k _{s,mean} [kN/mm]
taglio-trazione	0°	monotone	-	119,0	129,0	143,1	11,8
trazione a 45°	45°	monotone	141,0	140,6	151,7	160,4	21,0
		cicliche	-	162,5	171,2	180,0	23,6
trazione pura	90°	monotone	-	119,0	122,0	127,5	11,8
taglio a 45°	135°	monotone	97,0	101,0	107,5	114,9	33,0
		cicliche	-	101,9**	108,9**	126,1**	9,0**
taglio-compressione	180°	monotone	-	168,9	185,9	199,4	13,4
compressione a 45°	225°	miste***	-	207,7	254,1	289,7	23,0
compressione pura	270°	monotone	-	168,9	181,3	199,4	13,4
taglio a 45°	315°	monotone	97	101,0	107,5	114,9	33,2
		cicliche	-	101,9**	108,9**	126,1**	9,0**

Figure 36: Summary of the tests performed on the connection

Sollecitazione = Stress

Angolo = Angle

Note = Note

Taglio-trazione = shear-tension

Trazione a 45° = 45 degree tension

Trazione pura = pure tension

Taglio a 45° = 45 degree shear

Taglio-compressione = shear-compression

Compressione a 45° = 45 degree compression

Compressione pura = pure compression

Monotone = monotonic

Cicliche = cyclic

Miste = mixed

* The 45 degree compression tests were stopped at the maximum load of the hydraulic jack; the trend of the test in the Force-Displacement plane is basically linear up to that point. This allows to assume that the real resistance of the connection is much higher than the values seen in the tests.

4.3. Failure mode of the connection

As shown, the X-RAD connection system consists of a large number of basic components:

- 6 full thread VGS screws stressed axially and by shear, that perform the wood-to-wood connection between the CLT panel and the LVL insert of the X-ONE;

- an LVL insert, subjected to compression stress orthogonal to the fibre and to bearing stress by the internal bolts;
- 2 internal bolts, that connect the internal plate to the LVL insert, creating a wood-steel-wood shear connection;
- an external metal box, that envelops the LVL insert, that is subjected mainly to bearing stress at the bolts connecting it to the external plate;
- an internal plate, connected to the external plate and to the metal box by means of the two external bolts;
- 2 external bolts that connect the external plate to the internal plate and to the bent metal plate;
- a set of external plates called X-PLATES that allow for fastening to the ground or the mutual fastening between connections. The external plates have not been tested in this study.

Following are some pictures of the main components mentioned above.

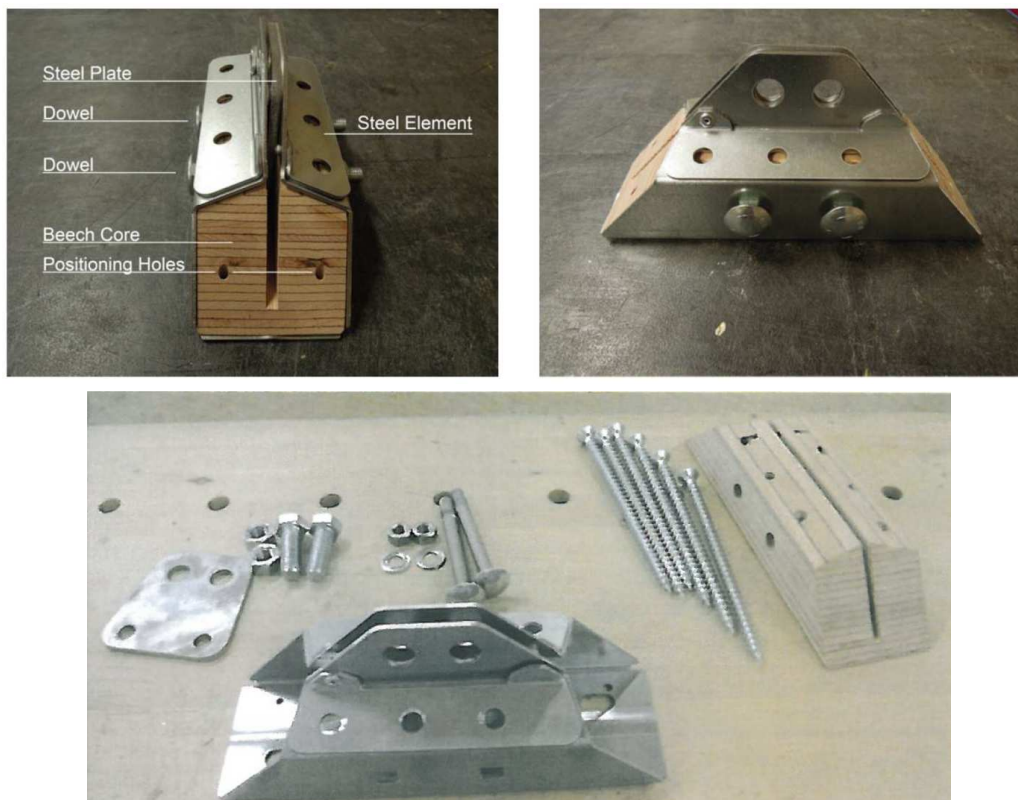


Figure 37: X-RAD system components

If one analyses the various resistance mechanisms, at least three elementary connections can be identified:

- wood-wood connection via the full thread screws. In turn, this connection can collapse via various failure modes:
 - a) screw failure in shear;
 - b) screw thread withdrawal from the CLT panel;
 - c) screw thread withdrawal from the LVL insert;

- wood-steel-wood bolted connection between the internal plate and the LVL insert. In turn, this connection can collapse via various failure modes:
 - a) wood-side failure of the bolt-LVL shear connection;
 - b) plate failure in bearing stress at the bolts;
- steel-steel bolted connection between the metal box + internal plate system and the external plate. In turn, this connection can collapse via various failure modes:
 - c) failure caused by bearing stress in correspondence with the bolts;
 - d) failure caused by "block-tearing".

The prototyping phase of the connection, however, has allowed to provide over-resistance to some of the collapse modes, so as to concentrate any failures on specific points:

- screw failure in shear at the wood-wood connection with full thread screws;
- "block tearing" of the metal box and of the internal plate in the metal box + internal plate/external plate connection.

It is important to define the failure mode of the connection subjected to generic stress, because the designer must define the pertinent safety factor.

The laboratory tests confirm the considerations made above. In fact, failure occurs as illustrated here below. For clarity purposes, following is a picture giving a definition of the various stresses.

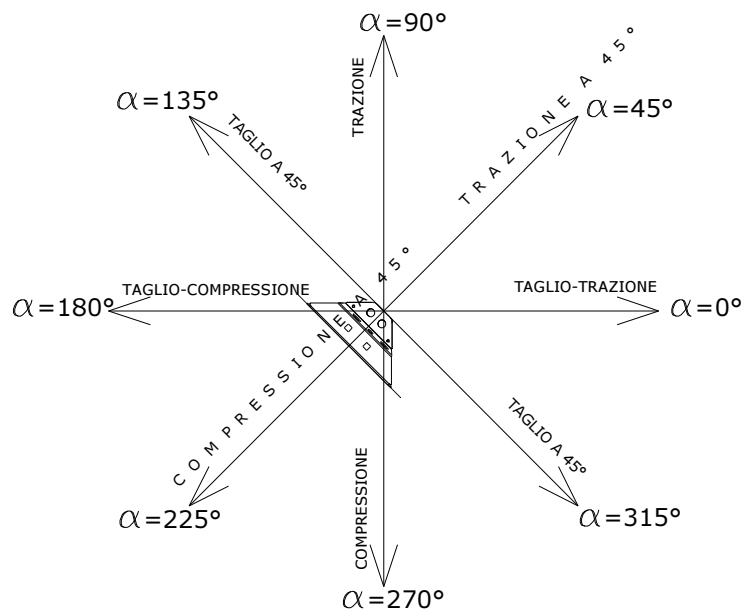


Figure 38: Stresses applied to the X-RAD in the CLT wall reference system

TRAZIONE = TENSION

TAGLIO A 45° = 45 DEGREE SHEAR

TAGLIO-TRAZIONE = SHEAR-TENSION

COMPRESSIONE = COMPRESSION

COMPRESSIONE A 45° = 45 DEGREE COMPRESSION

TAGLIO-COMPRESSIONE = SHEAR-COMPRESSION

4.3.1. Shear-Tension ($\alpha=0^\circ$)

Failure occurs by tension (shearing) at the VGS screws, and the collapse mechanism therefore is steel-side.

4.3.2. 45 degree tension ($\alpha=45^\circ$)

Failure occurs by block-tearing of the plates at the $\varnothing 16$ bolt holes. In detail, there is the simultaneous failure of the internal plate and of the metal box. The failure, therefore, involves a steel-side resistant mechanism.



Figure 39: Failure by block-tearing at $\varnothing 16$ holes

4.3.3. Tension ($\alpha=90^\circ$)

The configuration is the same as that of the shear-tension ($\alpha=0^\circ$) stress. This implies the same considerations, with steel-side failure at the screws.

4.3.4. 45 degree shear ($\alpha=135^\circ$ or $\alpha=315^\circ$)

Failure occurs by tension applied to the screws subjected to axial load. The failure mechanism, therefore, is steel-side.

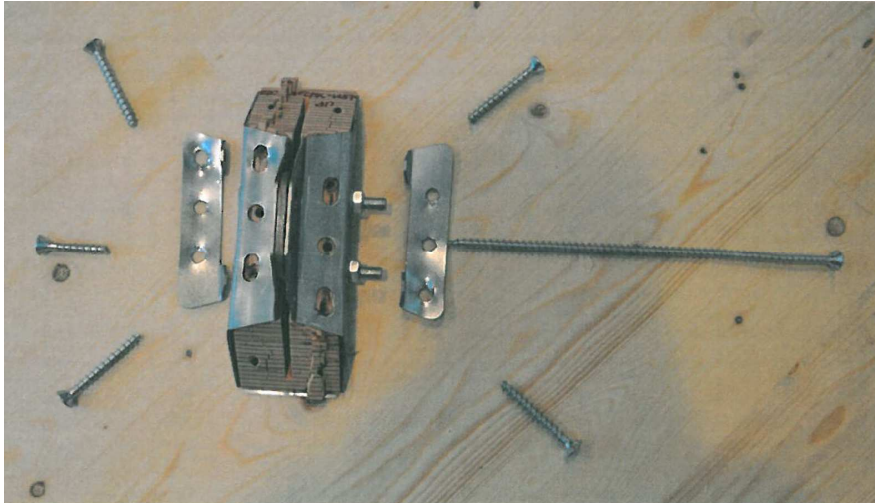


Figure 40: X-RAD driven to failure by 45 degree shear stress – notice shearing of screws.

4.3.5. Shear-Compression ($\alpha=180^\circ$)

In this case, failure occurs via mechanisms that can change according to test:

- Failure in tensile stress of the tensioned screws (i.e. steel-side shearing mechanism);
- Failure by withdrawal of the screw thread (i.e. wood-side mechanism);
- Failure by withdrawal of wood wedge, accompanied by splitting effects on the CLT panel (i.e. wood-side mechanism).

In the interests of safety, it is considered that these tests show wood-side failure, with use of the consequential safety factor.

4.3.6. 45 degree compression ($\alpha=225^\circ$)

Failure occurs by wood compression, possibly with failure by thread withdrawal from the LVL. The failure mechanism, therefore, is wood-side.

4.3.7. Compression ($\alpha=270^\circ$)

The configuration is the same as that of the shear-compression ($\alpha=0^\circ$) stress. This implies the same considerations, with wood-side failure.

4.4. Failure assessment

In order to extend further the investigation on the mechanical behaviour of the connection, an analytical calculation was conducted starting from the experimental analysis and analytically processing backwards the results obtained in accordance with the simplified static designs.

The assessment was made according to the *static theorem of limit analysis*, that allows to achieve an underestimation (i.e. in the interests of safety) of the collapse load of the connection. According to the static theorem, the structure does not arrive at the point of collapse under a system of loads in correspondence of which:

- There is a set of internal actions in balance with the loads.
- These internal actions fall within the admissibility domain, i.e. are compatible with the strength of the structural elements.

The definition of the equilibrium configuration to be analysed can be performed starting from the observation of experimental collapse modes so as to carry out a failure calculation based on the experimental failure mode.

As already seen above, the failure mechanisms involve the VGS screws or the steel plates with block-tearing type mechanisms.

Following are the limit diagrams hypothesised in the various stress configuration¹.

4.4.1. Shear-Tensile stress ($\alpha=0^\circ$)

When observing the samples pushed to failure, one notices breakage of the screws. The limit diagram hypothesised for the failure calculation is shown in the figure.

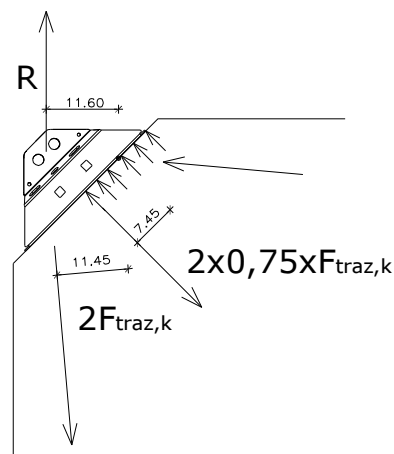


Figure 41: Shear-tension limit diagram

Legenda:

Traz. = Tens.

$$R_{u,k} = 111.6 \text{ kN}$$

¹ In some cases, the limit diagrams may seem rather bold, but their sole purpose is to attempt to analytically justify the actual mechanical behaviour highlighted during the experimental phase.

4.4.2. 45 degree tension ($\alpha=45^\circ$)

When observing the samples pushed to failure, two failure modes appear possible: screw-side, with the breakage of a pair of VGS screws, and steel-side, with the "block tearing" failure of the plates connected to the two $\varnothing 16$ bolts.

SCREW-SIDE FAILURE

The limit diagram used for the failure calculation is shown in the figure.

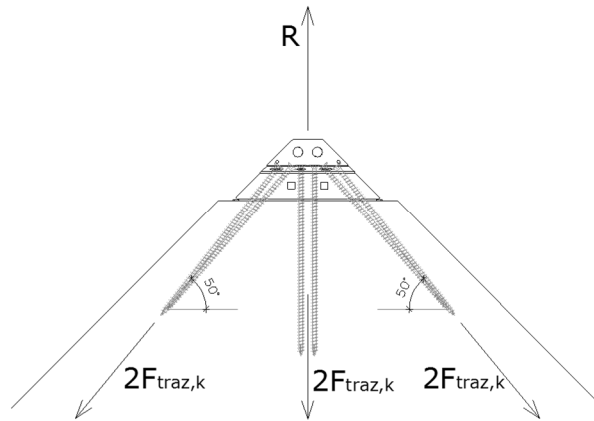


Figure 42: 45° tension limit diagram

Legenda:

Traz. = Tens.

There is a pair of screws inserted in a direction approximately parallel to the external load, while the other two pairs of screws are approx. 50° with respect to the external load. Upon failure, assuming perfect plasticity, the 3 pairs of screws shall be stressed by maximum loads, equal to:

$$R_{u,k} = 192.4 \text{ kN}$$

STEEL-SIDE FAILURE

Failure occurs by means of a "block-tearing" type mechanism, reference to which is made in item 3.10.2 of EN 1993-1-8 (Eurocode 3). The figure shows the diagram used for verification.

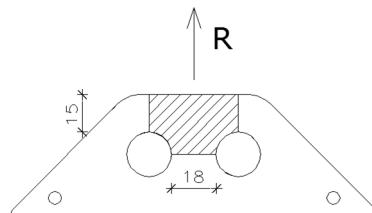


Figure 43: Block-tearing resistant mechanism

The characteristic resistance, by applying the suitable coefficients, is given by:

$$V_{eff,1,Rd} = \frac{410 \times 198}{\gamma_{M2}} + \frac{1}{\sqrt{3}} \frac{275 \times 330}{\gamma_{M0}} = \frac{81,18}{\gamma_{M2}} + \frac{852,39}{\gamma_{M0}}$$

CONNECTION RESISTANCE

The connection's resistance shall be the lowest of those seen in the foregoing. Considering the safety factors $\gamma_{M0}=1.05$ and $\gamma_{M2}=1.25$ envisaged in both Min. Decree No. 14-01-2008 and in EN 1995-1-1, the following design resistance results:

$$V_{eff,1,Rd} = \frac{81,18}{1,25} + \frac{52,39}{1,05} = 114,8 kN$$

As regards the wood-side failure, the following design resistance is obtained:

$$R_{u,d} = \frac{R_{u,k}}{\gamma_M} = \frac{192,4}{1,25} = 153,9 kN$$

As can be seen, the steel-side design resistance is lower to that of the wood side.

4.4.3. Tension ($\alpha=90^\circ$)

The geometric configuration, and therefore the resistance, is identical to that given for the shear-tension situation. Therefore, the resistance value is:

$$R_{u,k} = 111,6 kN$$

4.4.4. 45 degree shear ($\alpha=135^\circ$ or $\alpha=315^\circ$)

By observing the samples taken to failure, it is evident that failure occurs at the screws. The steel-side resistant mechanism is reported anyhow.

SCREW-SIDE FAILURE

A picture of the limit diagram used is shown.

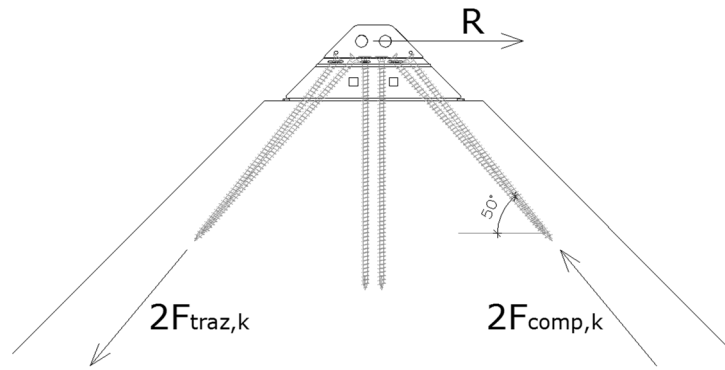


Figure 44: 45° shear limit diagram

Legenda:

Traz. = Tens.

Comp = Comp

It is assumed that the screws on the left are subjected to tension, those on the right to compression, and those in the middle to shear. In the interests of safety, the shear strength of the middle screws has been totally ignored, also because it is reasonable to presume that the shear strength of these screws occurs under much greater displacements than those compatible with the tensile strength of the other 4 screws.

The external breaking force is derived by projection of the four axial forces on the screws.

$$R_{u,k} = 93.9 \text{ kN}$$

STEEL-SIDE FAILURE

Failure occurs via a "block tearing" type mechanism, regarding which reference is made to item 3.10.2 of EN 1993-1-8 (Eurocode 3).

The diagram used for verification is shown in the following figure.

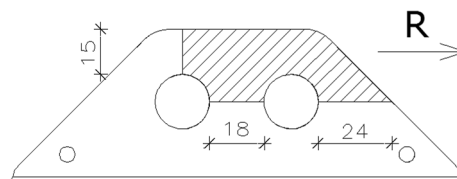


Figure 45: Block-tearing resistant mechanism

$$V_{eff,2,Rd} = \frac{0.5 \times 410 \times 165}{\gamma_{M2}} + \frac{1}{\sqrt{3}} \frac{275 \times 462}{\gamma_{M0}} = \frac{33.82}{\gamma_{M2}} + \frac{73.35}{\gamma_{M0}}$$

CONNECTION RESISTANCE

4.4.5. Shear-Compression ($\alpha=180^\circ$)

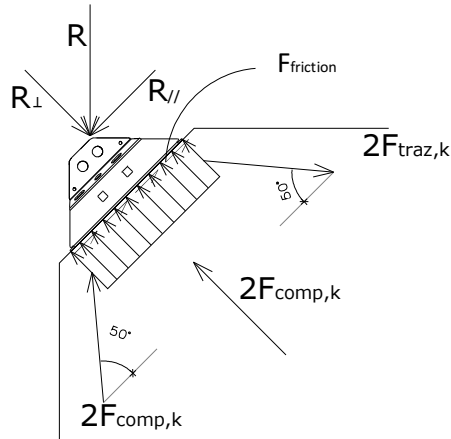


Figure 46: Shear-compression limit diagram

Legenda:

Traz. = Tens.

Comp = Comp

The total resistance is:

$$R_{u,k} = 165.9 \text{ kN}$$

4.4.6. 45 degree compression ($\alpha=225^\circ$)

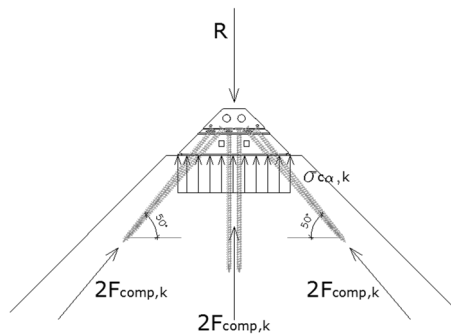


Figure 47: 45° compression limit diagram

Legenda:

Traz. = Tens.

Comp = Comp

The total resistance is:

$$R_{u,k} = 279.6 \text{ kN}$$

4.4.7. Compression ($\alpha=270^\circ$)

The geometric configuration, and therefore the resistance, is identical to that given for the shear-compression situation. Therefore, the resistance value is:

$$R_{u,k} = 165,9 \text{ kN}$$

5. DEFINITION OF A RESISTANCE CRITERION

Chapter 4 provides the calculation of the connection's resistance in the 8 most common geometrical configurations, corresponding to the 8 inclinations of the stresses. The purpose of this chapter is to derive a resistance criterion capable of covering the entire 360° spectrum.

5.1. Construction of the failure domain

The interaction domain, i.e the failure domain, is a plane figure in which all of the internal points represent load states that the connection is capable of withstanding. It can be demonstrated that the limit domain is always a convex, closed and limited figure. In other words, the closed figure that encloses the domain is a failure boundary, beyond which the connection's strength is overcome, while the points inside it are compatible with strength.

Three failure domains will be constructed in the following paragraphs, using three different methods:

- Experimental resistances;
- Resistances by FEM modeling;
- Resistances by analytical failure calculation.

5.1.1. Domain based on experimental resistances

The experimental resistances shown in Figure 45 can be represented in the X-Z plane as seen in Figure 44. Based on these precise values, it is possible to construct a diagram by interconnecting the various points. By joining the various points represented in this manner, one obtains a shear-tension (or shear-compression) interaction domain that is the failure boundary of the connection. This choice is supported by the considerations provided in the following paragraphs.

Coordinate dei punti del dominio di rottura sperimentale				
Sollecitazione sull'X-Rad	Angolo	R [kN]	Coordinate	
			V [kN]	N [kN]
taglio-trazione	0°	119,0	119,0	0,0
trazione a 45°	45°	141,0	99,7	99,7
trazione pura	90°	119,0	0,0	119,0
taglio a 45°	135°	97,0	-68,6	68,6
taglio-compressione	180°	168,9	-168,9	0,0
compressione a 45°	225°	289,7	-204,8	-204,8
compressione pura	270°	168,9	0,0	-168,9
taglio a 45°	315°	97,0	68,6	-68,6
taglio-trazione	360°	119,0	119,0	0,0

Figure 48: Experimental resistances of the connection

Legenda

Coordinate dei punti del dominio di rottura sperimentale = Coordinates of the experimental failure domain points

Sollecitazione sull'X-Rad = Stresses on the X-RAD

Angolo = Angle

Coordinate = Coordinates

Taglio-trazione = shear-tension

Trazione a 45° = 45 degree tension

Trazione pura = pure tension

Taglio a 45° = 45 degree shear

Taglio-compressione = shear-compression

Compressione a 45° = 45 degree compression

Compressione pura = pure compression

The diagram is shown in the following figure.

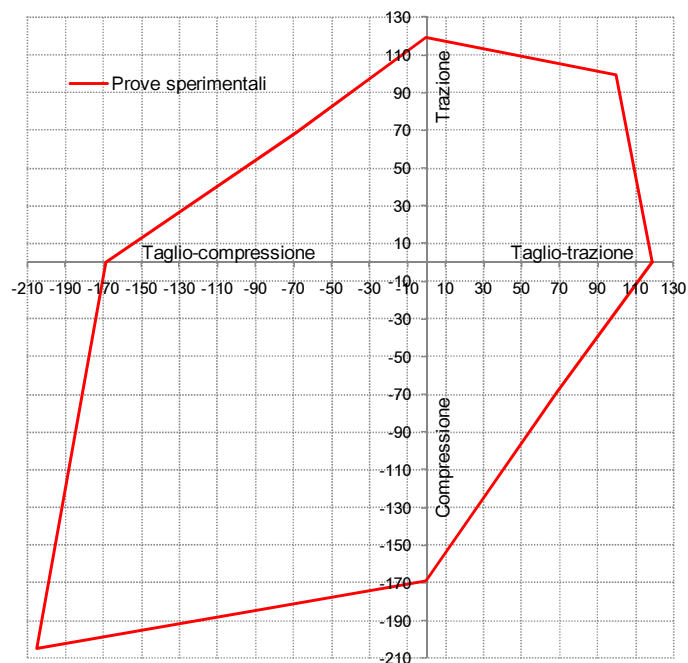


Figure 49: Experimental failure domain

Prove sperimentali = experimental tests

Taglio-compressione = shear-compression

Trazione = Tension

Taglio-trazione = shear-tension

Compressione = compression

The resulting failure domain can be used to perform a verification of the connection. By plotting the point that identifies the stress on this diagram, it is possible to make a graphic verification of the connection.

In fact, if the point that represents the stress lies within the failure domain, it means that the resistance verification has passed, while if the point is outside the domain, the verification has failed.

5.1.2. Domain based on resistances by FEM modeling

Figure 37 shows a diagram with FEM modeling resistances in the X-Y plane. By rotating and mirroring this diagram one obtains an interaction domain.

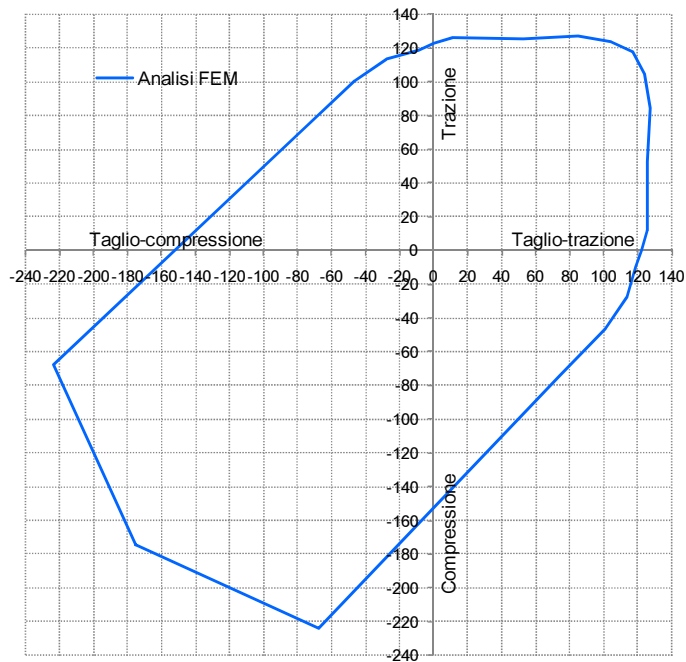


Figure 50: Failure domain from FEM analysis

Legenda:

Analisi FEM = FEM analyses

Taglio-compressione = shear-compression

Taglio-trazione = shear-tension

Compressione = compression

Trazione = tension

5.1.3. Comparison of experimental data with FEM modeling

By superimposing the two domains it is possible to make some observations.

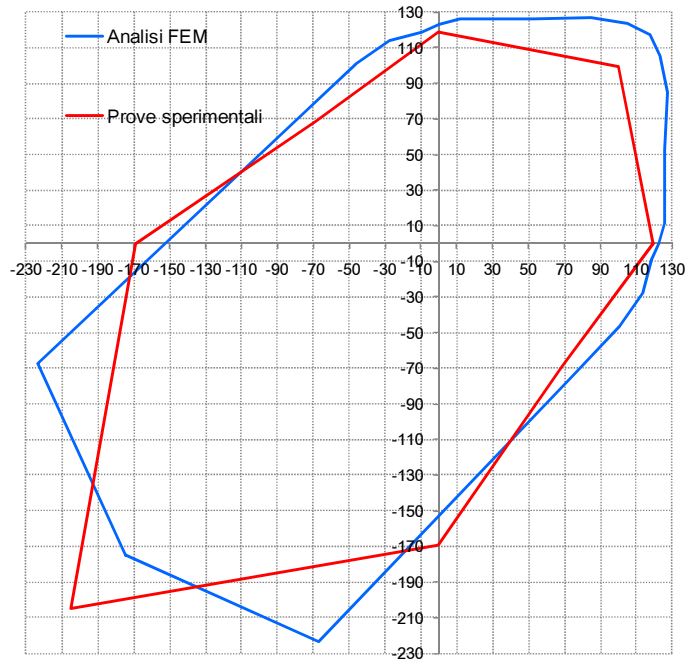


Figure 51: Superimposition of the two domains

Analisi FEM = FEM analyses

Prove sperimentali = Experimental tests

FEM modeling has allowed to perform virtual tests on the X-RAD connection, conducted at inclinations that are difficult to reproduce in a laboratory. The purpose of these tests was to interpolate the experimental results so as to reconstruct the interaction diagram in those areas not covered by the actual experimental investigations.

By observing the superimposition of the diagrams, one sees how, in this area of the plane (i.e. the upper right area), the diagram constructed starting from experimental investigations is always contained within the diagram deriving from the FEM analyses. This means that the linear trend hypothesised between one experimental value and the next is in favour of safety.

In the lower left quadrant of the domain, one notices a certain divergence between the trends of the two graphs, from which the following considerations can be inferred:

- The stress at 225° (45 degree compression) envisages the transfer of the force both by compression of the full thread screws within the CLT panel and by direct contact of the base of the X-ONE with the CLT panel's surface. These two transfer mechanisms, which work in parallel, are especially difficult to reproduce in a faithful manner.
- The stresses at 180° and at 270° (shear-tension and compression) envisage the transfer of a part of the X-RAD/CLT shear force via the force of friction. Friction has not been modeled, underestimating the connection resistance.

One can make a consideration, however, by observing that one of the two FEM analyses has been conducted at a 197° angle (and 253° by symmetry). This analysis shows, at a qualitative level, that between the angles of 180° and 225° (and between 225° and 270° by symmetry), the linear trend

used to interpolate the experimental data is significantly in the interests of safety. In these areas, in fact, the diagram based on FEM analysis is much 'wider' than that based on experimental tests.

In view of the foregoing, it can be stated that the choice of interpolating the experimental results with a linear trend between one test and the next is in the interests of safety.

5.1.4. Domain based on the resistances by analytical failure calculation

Following is a summary table listing the resistance values calculated using the analytical diagrams seen in the paragraphs above.

Sollecitazione sull'X-Rad	Angolo	R [kN]	Coordinate	
			V [kN]	N [kN]
taglio-trazione	0°	111,6	111,6	0,0
trazione a 45°	45°	133,6	94,4	94,4
trazione pura	90°	111,6	0,0	111,6
taglio a 45°	135°	93,9	-66,4	66,4
taglio-compressione	180°	165,9	-165,9	0,0
compressione a 45°	225°	279,6	-197,7	-197,7
compressione pura	270°	165,9	0,0	-165,9
taglio a 45°	315°	93,9	66,4	-66,4
taglio-trazione	360°	111,6	111,6	0,0

Figure 52: Analytical resistances of the connection

Sollecitazione sull'X-Rad =Stresses on the X-RAD

Angolo = Angle

Coordinate = Coordinates

Taglio-trazione = shear-tension

Trazione a 45° = 45 degree tension

Trazione pura = pure tension

Taglio a 45° = 45 degree shear

Taglio-compressione = shear-compression

Compressione a 45° = 45 degree compression

Compressione pura = pure compression

The resulting failure domain is shown here below.

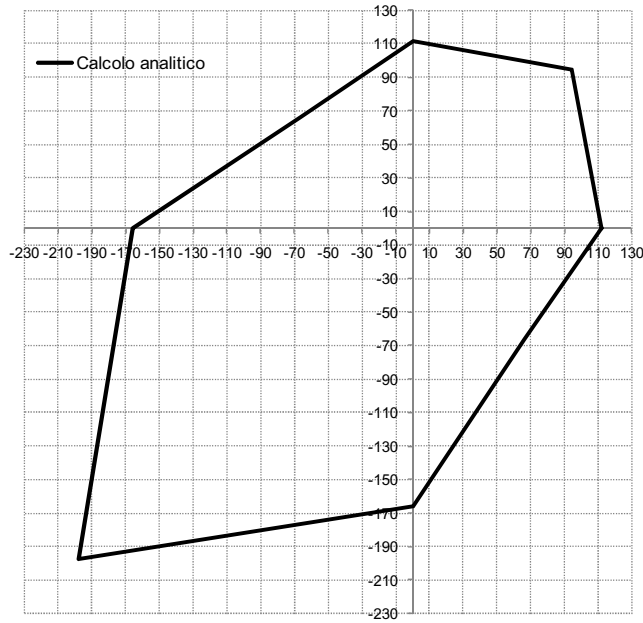


Figure 53: Interaction domain from analytical calculation

Calcolo analitico = analytical calculation

5.1.5. Comparison of experimental data with failure calculations

Shown is the superimposition of the experimental failure domain with the domain obtained from failure calculation. As can be seen, the analytical calculation domain is in every case in the interests of safety.

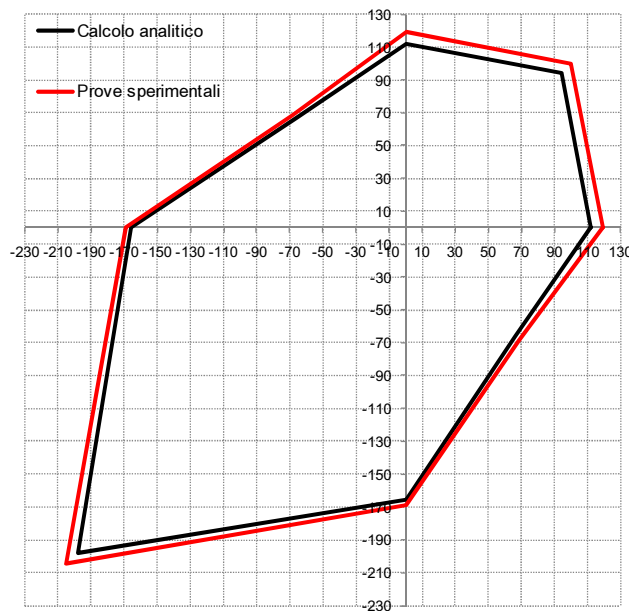


Figure 54: Superimposition of experimental domain on analytical calculation domain

Calcolo analitico = analytical calculation

Prove sperimentali = Experimental tests

5.1.6. Graphical interpretation of the domain

The following figure shows the characteristic resistance domain on which an image of the X-RAD connection has been superimposed. The picture helps to better comprehend to which stresses the various points on the domain correspond. In the figure, just by way of example, the vectors corresponding to the two stress states are shown.

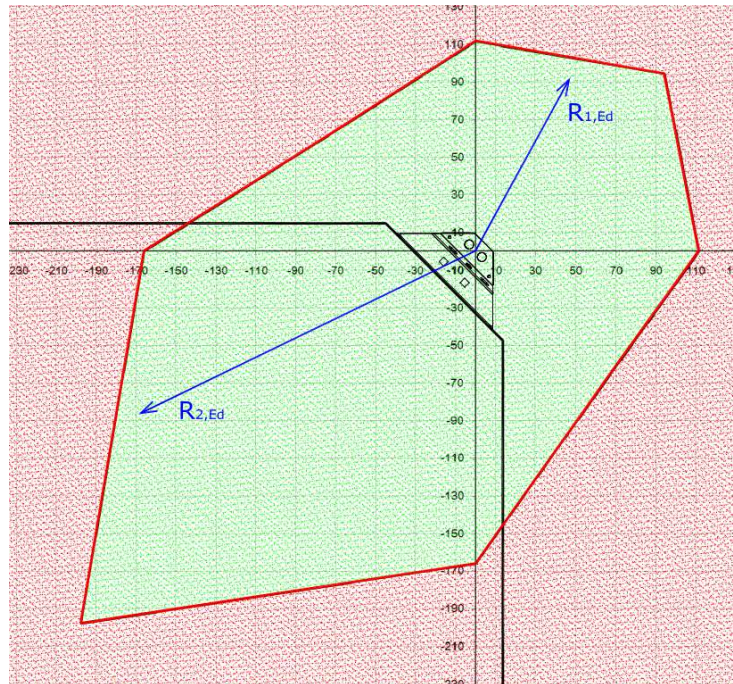


Figure 55: Graphical interpretation of the domain

5.2. Failure domain for the engineering designer

Starting from the characteristic failure domain of the connection, the engineer shall have to define a design failure domain so as to carry out the Ultimate Limit State resistance tests. The passage from the characteristic resistances to the design resistances varies according to whether the failure involves a wood connection (such as a wood-wood connection with full thread screws, for example) or a steel connection (such as a bolted connection between two steel plates, or the failure by tension of a screw). The passage from characteristic resistances to design resistances occurs in the following ways:

- **WOOD-SIDE FAILURE:** in this case, the formulas indicated in Chapter 4.4.6 of Min. Decree No. 14-01-2008 (*Technical Standards for Building Construction*), or in Chapter 2.4.1 of EN 1995-1-1 (Eurocode 5), shall apply:

$$R_d = k_{\text{mod}} \cdot \frac{R_k}{\gamma_M}$$

where:

$\gamma_M = 1,5$ pursuant to Min. Decree No. 14-01-2008 (IT);

$\gamma_M = 1,3$ pursuant to EN 1995-1-1 and EN 1998-1-1, for non-dissipative structural behaviour (Ductility class L);

$\gamma_M = 1,0$ pursuant to EN 1995-1-1 and EN 1998-1-1, for dissipative structural behaviour (Ductility classes M or H).

The pictures shown below, taken from European standards, more clearly explain the correct safety factor to be used for wood connections.

8.6 Safety verifications

1. (1)P The strength values of the timber material shall be determined taking into account the k_{mod} -values for instantaneous loading in accordance with EN 1995-1-1:2004.
2. (2)P For ultimate limit state verifications of structures designed in accordance with the concept of non-dissipative structural behaviour (Ductility class L), the partial factors for material properties for γ_M for the characteristics of the material used relating to the fundamental load combinations from EN 1995-1-1:2004 apply.
3. (3)P For ultimate limit state verifications of structures designed in accordance with the concept of dissipative structural behaviour (Ductility classes M or H), the partial factors for material properties γ_M for the characteristics of the material used relating to the fundamental load combinations from EN 1995-1-1:2004 apply.

Figure 56: Excerpted from UNI EN 1998-1-1

Table 2.3 – Recommended partial factors γ_M for material properties and resistances	
Fundamental combinations:	
Solid timber	1,3
Glued laminated timber	1,25
LVL, plywood, OSB	1,2
Particleboards	1,3
Fireboards, hard	1,3
Fireboards, medium	1,3
Fireboards, MDF	1,3
Fireboards, soft	1,3
Connections	1,3
Punched metal plate fasteners	1,25
Accidental combinations	1,0

Figure 57: Excerpted from UNI EN 1995-1-1

- **STEEL-SIDE FAILURE:** in this case the formulas indicated in 4.2.8.1.1 of Min. Decree No. 14-01-2008 (*Technical Standards for Building Construction*), or in Chapter 2.2 of EN 1993-1-8 (Eurocode 3) that envisage the use of the same safety factors, shall apply:

$$R_d = \frac{R_k}{\gamma_M}$$

In this case, a different safety factor shall be used in function of the failure type:

$\gamma_M = \gamma_{M0} = 1,05$ for the resistance, as regards the failure, of tensioned sections;

$\gamma_M = \gamma_{M2} = 1,25$ for the resistance of sections in general.

The following table summarises the experimental failure modes in the various stress configurations:

Modalità di rottura				
Sollecitazione sull'X-Rad	Angolo	Rottura	γ_M	k_{mod}
taglio-trazione	0°	Trazione delle viti (lato acciaio)	$\gamma_{M2}=1,25$	-
trazione a 45°	45°	Block tearing della piastra interna sui fori $\Phi 16$	$\gamma_{M0}=1,05$; $\gamma_{M2}=1,25$	-
trazione pura	90°	Trazione delle viti (lato acciaio)	$\gamma_{M2}=1,25$	-
taglio a 45°	135°	Trazione delle viti (lato acciaio)	$\gamma_{M2}=1,25$	-
taglio-compressione	180°	Rottura lato legno - estrazione del filetto delle viti	$\gamma_{M, legno}=1,5$ (1,3 secondo EC5)	1,0
compressione a 45°	225°	Rottura a compressione lato legno	$\gamma_{M, legno}=1,5$ (1,3 secondo EC5)	1,0
compressione pura	270°	Rottura lato legno - estrazione del filetto delle viti	$\gamma_{M, legno}=1,5$ (1,3 secondo EC5)	1,0
taglio a 45°	315°	Trazione delle viti (lato acciaio)	$\gamma_{M2}=1,25$	-
taglio-trazione	360°	Trazione delle viti (lato acciaio)	$\gamma_{M2}=1,25$	-

Figure 58: Failure mode of the connection

Modalità di rottura = Failure modes

Sollecitazione sull'X-Rad = Stresses on the X-RAD

Angolo = Angle

Rottura = Failure

Taglio-trazione = shear-tension

Trazione a 45° = 45 degree tension

Trazione pura = pure tension

Taglio a 45° = 45 degree shear

Taglio-compressione = shear-compression

Compressione a 45° = 45 degree compression

Compressione pura = pure compression

Taglio a 45° = 45 degree shear

Taglio-trazione = shear-tension

Trazione delle viti (lato acciaio) = Screw tension (steel side)

Block tearing della piastra interna sui fori $\Phi 16$ = Block tearing of internal plate at $\Phi 16$ holes

Trazione delle viti (lato acciaio) = Screw tension (steel side)

Trazione delle viti (lato acciaio) = Screw tension (steel side)

Rottura lato legno – estrazione del filetto delle viti = Wood side failure – withdrawal of screw thread

Rottura a compressione lato legno = Compression failure wood side

Rottura lato legno – estrazione del filetto delle viti = Wood side failure – withdrawal of screw thread

Trazione delle viti (lato acciaio) = Screw tension (steel side)

Trazione delle viti (lato acciaio) = Screw tension (steel side)

$\gamma_{M, legno} = (\gamma_{M, timber} = 1,5$ (1,3 by EC5)

5.2.1. Field of use of the connection

The connection based on X-ONE acts as a connection between CLT walls to prevent their overturning and displacement caused by seismic forces and by wind (instantaneous duration class). The vertical static forces are mostly transmitted directly via wall-to-wall contact, without stressing the connection. The use of X-ONE for short, medium or permanent duration loads ($k_{mod} < 1$) requires the designer's reevaluation of the design domain, since the hierarchy of the resistances could change. In these cases, in the interests of safety, design resistances can all be treated as wood-side resistances, allowing the application of the relating k_{mod} and γ_M factors.

At the moment no experimental data with short-term, medium-term or permanent applied loads are available, since the EN 26891:1991 prescribes the execution of "quasi-instantaneous" tests.

The considerations illustrated in this paragraph refer to the use of X-RAD for instantaneous duration loads. Should it be required to use X-RAD for short, medium or permanent duration class loads ($k_{mod} < 1$), the designer shall evaluate the γ_M and k_{mod} factors to be used.

5.2.2. Characteristic failure domain

The following paragraphs illustrate 3 failure domains:

- one based on experimental tests;
- one based on FEM analyses;
- one based on analytical diagrams.

The three domains are shown here.

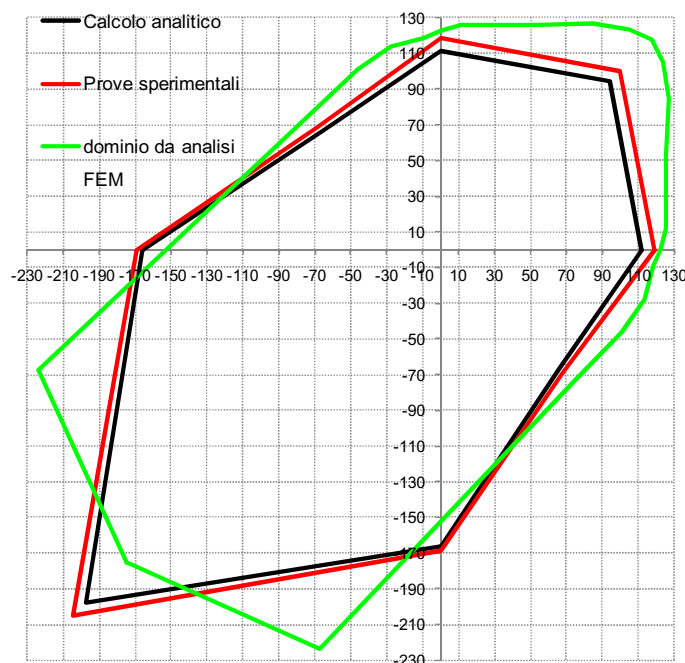


Figure 59: Superimposition of the three domains

Calcolo analitico = analytical calculation

Prove sperimentali = Experimental tests

Dominio da analisi FEM = Domain from FEM analysis

The characteristic failure domain is, therefore:

Sollcitazione sull'X-Rad	Angolo	R _k [kN]	Coordinate	
			V _k [kN]	N _k [kN]
taglio-trazione	0°	111,6	111,6	0,0
trazione a 45°	45°	141,0	99,7	99,7
trazione pura	90°	111,6	0,0	111,6
taglio a 45°	135°	97,0	-68,6	68,6
taglio-compressione	180°	165,9	-165,9	0,0
compressione a 45°	225°	279,6	-197,7	-197,7
compressione pura	270°	165,9	0,0	-165,9
taglio a 45°	315°	97,0	68,6	-68,6
taglio-trazione	360°	111,6	111,6	0,0

Figure 60: Characteristic failure domain

Sollcitazione sull'X-Rad = Stresses on the X-RAD

Angolo = Angle

Coordinate = Coordinates

Taglio-trazione = shear-tension

Trazione a 45° = 45 degree tension

Trazione pura = pure tension

Taglio a 45° = 45 degree shear

Taglio-compressione = shear-compression

Compressione a 45° = 45 degree compression

Compressione pura = pure compression

The resulting failure domain is shown in the following figure.

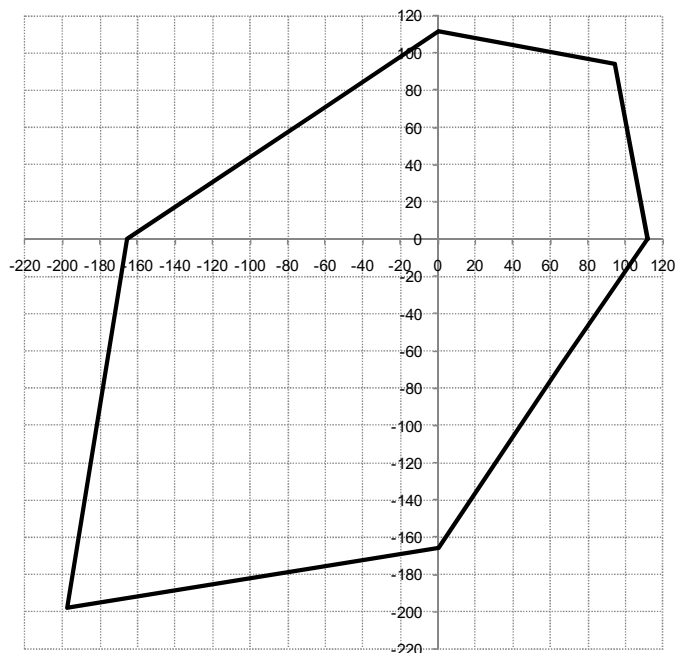


Figure 61: Characteristic failure domain

5.2.3. Design failure domain

Based on the characteristic domain seen here above and using the safety factors seen further above, it is possible to obtain the following resistance domain. The calculation in compliance with the Italian (Min. Decree No. 14-01-2008) and European (EN 1995-1-1) standards is also given.

Dominio di rottura di progetto - D.M. 14-01-2008						
Sollecitazione sull'X-RAD	Angolo	γ_M	k_{mod}	R_d [kN]	Coordinate	
					V_d [kN]	N_d [kN]
taglio-trazione	0°	1,25	-	89,3	89,3	0,0
trazione a 45°	45°	1,25*	-	112,8	79,8	79,8
trazione pura	90°	1,25	-	89,3	0,0	89,3
taglio a 45°	135°	1,25	-	77,6	-54,9	54,9
taglio-compressione	180°	1,50	1,0	110,6	-110,6	0,0
compressione a 45°	225°	1,50	1,0	186,4	-131,8	-131,8
compressione pura	270°	1,50	1,0	110,6	0,0	-110,6
taglio a 45°	315°	1,25	-	77,6	54,9	-54,9
taglio-trazione	360°	1,25	-	89,3	89,3	0,0

Figure 62: Design resistances – Min. Decree No. 14-01-2008

Legenda:

Dominio di rottura progetto – D.M. 14-01-2008 = Design failure domain – Min. Decree No. 14-01-2008

Sollecitazione sull'X-Rad = Stresses on the X-RAD

Angolo = Angle

Coordinate = Coordinates

Taglio-trazione = shear-tension

Trazione a 45° = 45 degree tension

Trazione pura = pure tension

Taglio a 45° = 45 degree shear

Taglio-compressione = shear-compression

Compressione a 45° = 45 degree compression

Compressione pura = pure compression

Taglio a 45° = 45 degree shear

Taglio-trazione = shear-tension

Dominio di rottura di progetto - EN 1995-1-1 + EN 1998-1-1						
Solllecitazione sull'X-RAD	Angolo	γ_M	k_{mod}	R [kN]	Coordinate	
					V [kN]	N [kN]
taglio-trazione	0°	1,25	-	89,3	89,3	0,0
trazione a 45°	45°	1,25*	-	112,8	79,8	79,8
trazione pura	90°	1,25	-	89,3	0,0	89,3
taglio a 45°	135°	1,25	-	77,6	-54,9	54,9
taglio-compressione	180°	1,30**	1,1	140,4	-140,4	0,0
compressione a 45°	225°	1,30**	1,1	236,6	-167,3	-167,3
compressione pura	270°	1,30**	1,1	140,4	0,0	-140,4
taglio a 45°	315°	1,25	-	77,6	54,9	-54,9
taglio-trazione	360°	1,25	-	89,3	89,3	0,0

Figure 63: Design resistances - EN 1995-1-1

Legenda:

Dominio di rottura di progetto – EN 1995-1-1 + EN 1998-1-1 = Design failure domain – EN 1995-1-1 + EN 1998-1-1

Solllecitazione sull'X-Rad = Stresses on the X-RAD

Angolo = Angle

Coordinate = Coordinates

Taglio-trazione = shear-tension

Trazione a 45° = 45 degree tension

Trazione pura = pure tension

Taglio a 45° = 45 degree shear

Taglio-compressione = shear-compression

Compressione a 45° = 45 degree compression

Compressione pura = pure compression

Taglio a 45° = 45 degree shear

Taglio-trazione = shear-tension

* *both safety factors should be used for the steel-side resistant mechanism (block tearing). Having considered the resistance from the ETA, based on experimental investigations, it is impossible to break down the block-tearing strength into the two basic components (shear and tensile stress). For this reason, in the interests of safety, a single safety factor is used, equivalent to γ_{M2} . N.B. Had the connection strength been wood side, if the European standard were applied, a safety factor of $\gamma_M=1.00$ could have been used, since the ductility class for 45 degree tension declared by the ETA is equal to M.*

** *as regards wood connections, EN 1998-1-1 allows for the use of the $\gamma_M=1.00$ factor relating to accidental combinations only if the connection's ductility class is M or H. In the case of ductility class L, the $\gamma_M=1.30$ factor relating to static combinations must be used. As regards angles 180°, 225° and 270°, the ETA does not provide a ductility class. Thus, in the interests of safety, a ductility class L with factor $\gamma_M=1.30$ is considered. Conversely, Italian legislation does not mention any difference of γ_M in function of ductility class, and therefore considers $\gamma_M=1.50$.*

The following graph shows two design domains, together with the characteristic domain. The difference between the design domains in the case of stresses at angles 180°, 225° and 270°, for

which the failure occurs wood-side, is clear. In this case, the Italian and the European standards follow two different paths.

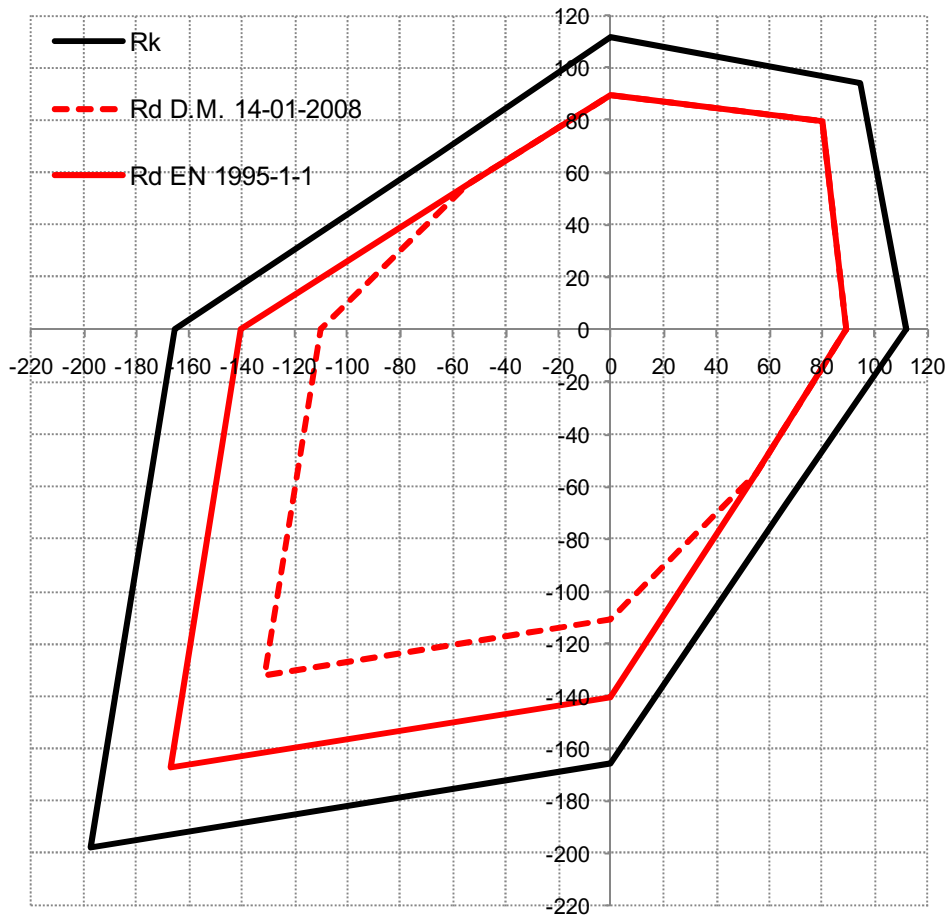


Figure 64: Design domains

5.3. Design provisions as per European Technical Approval (ETA- 15/0632)

The European Technical Approval (ETA) currently being issued provides several indications regarding the expected utilisation of the connection:

- X-RAD can be used for connecting CLT elements.
- X-RAD can be subjected to static, quasi-static or seismic actions.
- X-RAD can be used with service classes 1 or 2, in accordance with EN 1995-1-1.

As regards connection designing, the ETA states that:

1. The designing of X-RAD connections must be conducted under the responsible supervision of an engineer experienced in timber building construction.
2. The designing of the works must ensure the protection of the connections, so as to maintain service classes 1 or 2 in accordance with EN 1995-1-1.
3. The X-RAD connections must be installed correctly.

4. The absence of splitting phenomena must be verified, in accordance with EN 1995-1-1.

5.3.1. Splitting

This last prescription deserves further attention. During the execution of the tests, and more specifically in proximity of the failure of the samples, more or less marked splitting phenomena were observed. In turn, these phenomena involved the opening of the CLT panel in correspondence with the pair of screws most subjected to tensile stress, with the extraction of a wood wedge. The resistances derived from the tests were therefore determined in the presence of splitting. Despite this, the ETA prescribes particular care in avoiding the occurrence of these phenomena.

For this reason, it is suggested that, in the event that the connection be especially designed to exploit its performance in terms of resistance, screws be inserted in the direction perpendicular to the panel's axis (e.g.: VGZ $\varnothing 7$ screws), so as to "sew" it, thus acting as reinforcement against the onset of splitting. The effect of this precaution would be to shift the ultimate strength upwards, leading the connection to fail by screw tension, so as to fully exploit its resistance. A graphical diagram showing the positioning of the reinforcement screws is as follows.

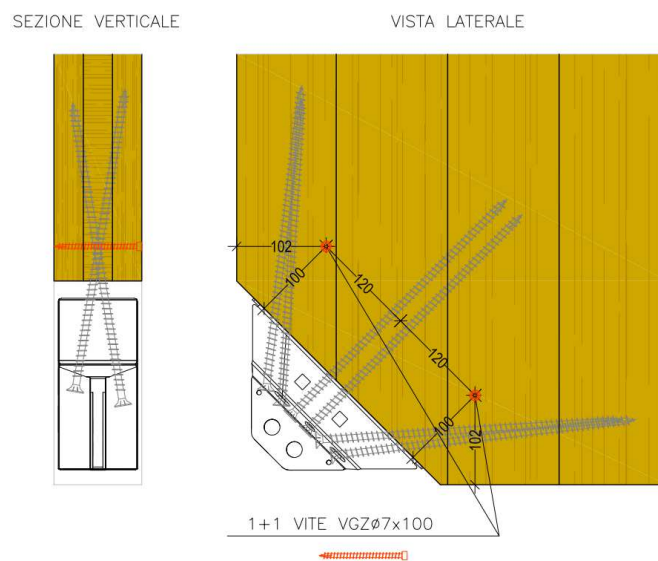


Figure 65: Reinforcement screws against splitting

SEZIONE VERTICALE = VERTICAL SECTION

VISTA LATERALE = SIDE VIEW

1+1 VITE VGZ $\varnothing 7 \times 100$ = 1+1 VGZ SCREW $\varnothing 7 \times 100$

The original document is written in Italian. Versions in other languages derive from this original document